**Geomechanics and Engineering**, *Vol. 27, No. 1 (2021) 13-30*
https://doi.org/10.12989/gae.2021.27.1.013


# Review on engineering properties of MICP-treated soils

Tong Yu[1a], Hanène Souli[2b], Yoan Pechaud[3c] and Jean-Marie Fleureau*[1]

[1]*Laboratoire de Mécanique des Sols, Structures et Matériaux, CNRS UMR 8579, Université Paris Saclay, CentraleSupélec, 8-10 Rue Joliot Curie, 91190 Gif-sur-Yvette, France*
[2]*Laboratoire de Tribologie et Dynamique des Systèmes, CNRS UMR 5513, Université de Lyon, CentraleLyon-ENISE, 58 Rue Jean Parot, 42023 Saint Etienne Cedex, France*
[3]*Laboratoire Géomatériaux et Environnement, Université Gustave Eiffel, 77454 Marne-la-Vallée Cedex 2, France*

*(Received July 24, 2020, Revised September 15, 2021, Accepted September 28, 2021)*

**Abstract.** Microbial induced calcium carbonate precipitation (MICP), a sustainable and effective soil improvement method, has experienced a burgeoning development in recent years. It is a bio-mediated method that uses the metabolic process of bacteria to cause $CaCO_3$ precipitation in the pore space of the soil. This technique has a large potential in the geotechnical engineering field to enhance soil properties, including mitigation of liquefaction, control of suffusion, etc. Multi-scale studies, from microstructure investigations (microscopic imaging and related rising techniques at micron-scale), to macroscopic tests (lab-based physical, chemical and mechanical tests from centimeter to meter), to in-situ trials (kilometers), have been done to study the mechanisms and efficiency of MICP. In this article, results obtained in recent years from various testing methods (conventional tests including unconfined compression tests, triaxial and oedometric tests, centrifuge tests, shear wave velocity and permeability measurements, as well as microscopic imaging) were selected, presented, analyzed and summarized, in order to be used as reference for future studies. Though results obtained in various studies are rather scattered, owning to the different experimental conditions, general conclusions can be given: when the $CaCO_3$ content (CCC) increases, the unconfined compression strength increases (up to 1.4 MPa for CCC=5%) as well as the shear wave velocity (more than 1-fold increase in $\boldsymbol{V_s}$ for each 1% $CaCO_3$ precipitated), and the permeability decreases (with a drop limited to less than 3 orders of magnitude). Concerning the mechanical behavior of MICP treated soil, an increase in the peak properties, an indefinite increase in friction angle and a large increase in cohesion were obtained. When the soil was subjected to cyclic/dynamic loadings, lower pore pressure generation, reduced strains, and increasing number of cycles to reach liquefaction were concluded. It is important to note that the formation of $CaCO_3$ results in an increase in the dry density of the samples, which adds to the bonding of particles and may play a major part in the improvement of the mechanical properties of soil, such as peak maximum deviator, resistance to liquefaction, etc.

**Keywords:** biocementation; engineering properties; microstructures; MICP

## 1. Introduction

Microbial induced calcium carbonate precipitation (MICP) is a novel, sustainable, cost-competitive soil improvement technique with a low-$CO_2$ emission (Røyne *et al.* 2019). It has known a great development in the past decade, in the exploration of protocols (Yu *et al.* 2020), engineering properties and up-scaling applications. The process of MICP is schematically shown in Fig. 1. The method benefits from the metabolic process of microorganisms, such as *Sporosarcina pasteurii* (*S. pasteurii*), a ubiquitous, non-toxic and effective strain often used in practice. This strain can produce an enzyme – urease – that enhances the hydrolysis process of urea. Ammonium and carbonate ions are produced. With the presence of $Ca^{2+}$ ions, the resulting crystals of $CaCO_3$ can precipitate on the surface and in the pore throats of soil grains, which in return improves the soil engineering properties by forming bonds between soil particles and increasing their surface roughness. These properties include physical, conduction, mechanical properties, and chemical composition (Dejong *et al.* 2013).

MICP is promising in many geotechnical engineering fields, as summarized in some existing review articles (Ivanov and Chu 2008, Dejong *et al.* 2010). Studies of MICP, related to liquefaction mitigation (Montoya *et al.* 2012, Wu 2015, Xiao *et al.* 2018), stability and erosion control of slopes, dams and coastal area (Jang *et al.* 2017, Do *et al.* 2019, Haouzi *et al.* 2019, Imran *et al.* 2019), wind erosion and dust control (Bahmani *et al.* 2017, Li *et al.* 2018), crack repair in concrete and mortar (Choi *et al.* 2017, Son *et al.* 2018), etc., have proved the effectiveness of this method. It can also be a good choice if the local soil is not suitable for conventional treatment methods like injecting cement or chemicals. Due to these prospective applications,

*Corresponding author, Professor
E-mail: jean-marie.fleureau@centralesupelec.fr
[a]Ph.D. Student
E-mail: tong.yu@centralesupelec.fr
[b]Associate Professor
E-mail: hanene.souli@enise.fr
[c]Associate Professor
E-mail: yoan.pechaud@u-pem.fr



ISSN: 2005-307X (Print), 2092-6219 (Online)

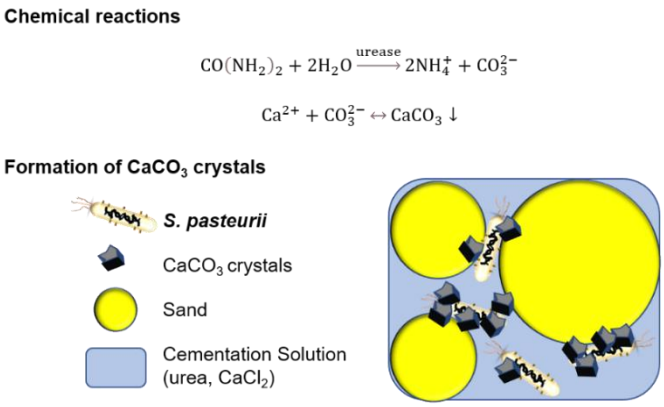


Fig. 1 Schematic diagram of MICP process

researchers have carried out multi-scale studies using different testing methods to study the mechanisms and efficiency of MICP, from microscopic analyses to macroscopic tests and in-situ trials. Results of lab-based tests on MICP-treated soils highlight the enhanced soil behavior under either monotonic or dynamic loading. Meanwhile, microscopic studies give a more thorough knowledge of the role of microbes and $CaCO_3$ crystals in the MICP process.

In the past reviews concerning MICP method, processes, and applications, comparison among different soil improvement methods were well summarized (e.g., Ivanov and Chu 2008, Dejong *et al.* 2010, Wang *et al.* 2017). Recently, a review by Choi *et al.* (2020) brought out very interesting quantitative data about microscopic and macroscopic properties of MICP-treated soils. However, in terms of engineering properties of MICP-treated soils, there is still a need for analysis and synthesis of the fast-growing experimental results for the future development of MICP technique. The objective of the present review is therefore to analyze critically the behavior of MICP-treated soils under monotonic and dynamic loadings. Some crucial engineering properties such as unconfined compression strength, compressibility coefficient, friction angle, cohesion, shear wave velocity and permeability are discussed precisely and incisively, and presented as a function of $CaCO_3$ content. Results from microscopic studies are also provided to better understand the micro-mechanisms that are of great significance to improve the efficiency of the method and engineering behavior of MICP-treated soils. At the end of the article, some interesting and useful conclusions and expectations are provided for future reference.

## 2. Testing methods and mechanical properties of bio-cemented soils

In this section, engineering properties of bio-cemented soil were summarized and analyzed on the base of various tests, including monotonic/cyclic loading tests and measurements of shear wave velocity and permeability.

### *2.1 Unconfined compression tests*

Unconfined compression test is a simple and fast way to measure the strength of soil samples. Unconfined compression strength (UCS) is widely used for rapid comparison of the strength of MICP-treated samples that are fabricated using different protocols. Fig. 2(a) shows the change in UCS as a function of the percentage of deposited calcium carbonate for various sands of the literature. The median diameter of the grains ($d_{50}$) used in these studies, as well as the uniformity coefficient $C_u$, are reported in Fig. 2(b) as an indication of the grain size distributions. There is a large scatter in the values of UCS for a given percentage of carbonate.

The change in UCS in saturated specimens depends on several parameters, e.g. (i) the percentage of carbonate, (ii) the repartition of the $CaCO_3$ crystals in the porous medium, (iii) the adhesion of the crystals on particles. In granular soils, the standardized minimum and maximum void ratios mainly depend on the uniformity coefficient and grain shape (Biarez and Hicher 1994). This means that, under similar conditions of uniformity coefficients, relative densities, and grain shapes, the void ratio of the soil remains constant, independently of the size of the grains. Therefore, the percentage of calcium carbonate necessary to obtain a similar filling of the voids is independent of the size of the grains and should therefore produce a similar effect on the unconfined compression strength. Fig. 2 confirms this assumption as, for the same carbonate content, the UCS of the coarse sand of Gomez and Dejong (2017) are very high whereas those of the aggregates of Mahawish *et al.* (2018) are very low. The reason is probably different repartitions of the crystals in the soil.

Another parameter that must be taken into account is the saturation of the tested specimens. Unsaturation results in the existence of a suction within the soil and leads to an increase in strength due to capillary and adsorption phenomena (e.g., Taibi *et al.* 2008). In fine sands, this capillary effect may be very important and affect the results as it is impossible to separate the role of cementation from that of saturation. In most of UCS tests, the degree of saturation can be assumed to be lower than 1 but, unfortunately, this parameter is never mentioned in the papers, and this contributes to the scatter of the results.

Concerning the influence of the uniformity coefficient $C_u$, it is well established that the standardized minimum and maximum void ratios decrease when $C_u$ increases from 1 to 10, and remain more or less constant afterwards. As a

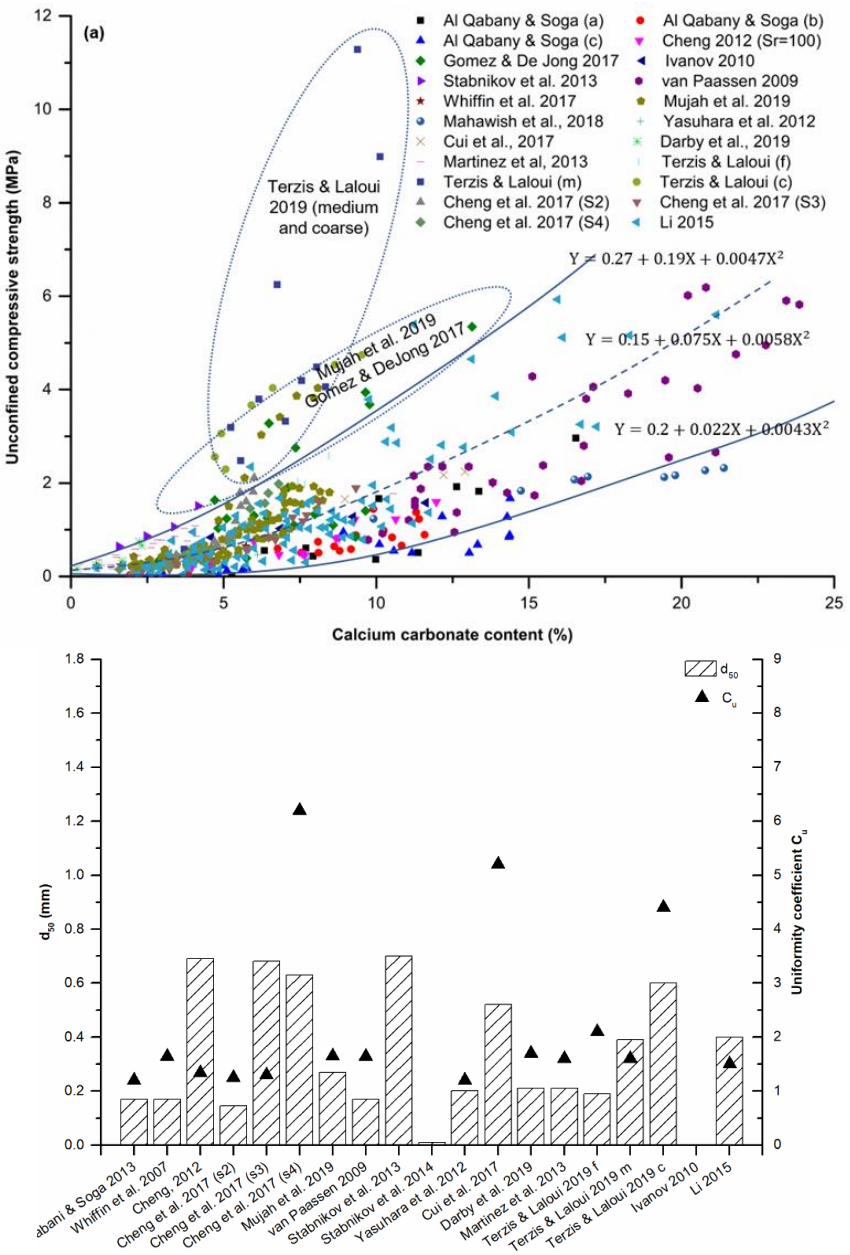


Fig. 2 (a) Unconfined compressive strength as a function of calcium carbonate content for various papers of the literature; (b) Medium diameter $d_{50}$ and uniformity coefficient $C_u$ for the different soils reported above

consequence, for a given relative density (and grain shape factor), the soil will be denser if $C_u$ is larger. For most of the tested soils, the relative density is high enough (larger than 50%, mostly around 80-90%), so that this parameter plays a limited part. It appears in Fig. 2(a) that the soils with the highest uniformity coefficient (i.e., the sand S4 of Cheng *et al.* (2017), the sand (b) of Gomez and Dejong (2017), that of Cui *et al.* (2017) and the sand (c) of Terzis and Laloui (2019) are predominantly located above the main bulk of samples. For the other soils, the value of $C_u$ seldom exceeds 2. This observation is consistent with the remarks of several researchers (e.g., Martinez and Dejong 2009, Terzis and Laloui 2019) who noted that, at a given calcium carbonate percentage, the densest specimens featured the highest UCS because they had a larger number of contact points between particles where the crystals could form. In fact, the spreading of the grading curves (characterized by $C_u$) seems to be much more important than the maximum size of the grains.

Considering now all the points of Fig. 2(a), it appears that most points are comprised between the two continuous curves with parabolic shapes, with a mean value represented by the dashed line. Note that, up to 8% of calcium carbonate content, the experimental points are located equally on both sides of the dashed line whereas, for larger $CaCO_3$ contents, the points are predominantly between the dashed line and the lowest line, and even below the latter. However, three family of results are mostly out of the previous range: those of Gomez and Dejong (2017), Mujah *et al.* (2019) and Terzis and Laloui (2019), surrounded by ellipses in Fig. 2(a). The information present in the papers does not allow to understand or explain the

Table 1 Parameters of the shear wave velocity tests in the literature

| Reference | Bacteria | Sand | $d_{50}$ (mm) | Relative density | $C_u$ | Confining pressure (kPa) |
|---|---|---|---|---|---|---|
| (Weil *et al.* 2012) | *S. pasteurii* | Ottawa 50-70 | 0.12 | 40-60 | 1.4 | 100 |
| | | Ottawa 20-30 | 0.7 | | 1.17 | |
| (Martinez *et al.* 2013) | *S. pasteurii* | Ottawa 50-70 | 0.21 | 78-100 | 1.4 | 100 |
| (Montoya *et al.* 2013) | *S. pasteurii* | Ottawa 50-70 | 0.22 | 40 | 1.4 | - |
| (Dejong *et al.* 2014) | *S. pasteurii* | Ottawa 50-70 | 0.21 | 84 | 1.4 | - |
| (Lin *et al.* 2016) | *S. pasteurii* | Ottawa 50-70 | 0.33 | 41 | 1.43 | 25, 50, 100 |
| | | Ottawa 20-30 | 0.71 | 39 | 1.17 | |
| (Montoya and Dejong 2015) | *S. pasteurii* | Ottawa 50-70 | 0.22 | 31-45 | 1.4 | 100 |
| (Feng and Montoya 2017) | *S. pasteurii* | Ottawa 50-70 | 0.22 | 38 | 1.4 | 100 |
| (O'Donnell *et al.* 2017) | Denitrifying bacteria | Ottawa 20-30 | *0.85 | 21-51 | - | 3 |
| | | Huntington beach sand | 0.55 | 67 | - | |
| (Gomez and Dejong 2017) | Native soil microorganism | SM | *0.15 | 50-65 | 2.3 | 60, 100 |
| | | SP | *0.97-1.59 | | 6.6-10.1 | |
| | | | *0.26 | | 7.7 | |
| | | | *1.95 | | 1.6 | |
| | | SP-SC | *0.38-0.51 | | 4.4-7.3 | |
| | | SP-SM | *0.21-0.28 | | 3.2-3.6 | |
| (Gomez *et al.* 2018) | Native soil microorganism | Concrete sand | - | - | - | - |
| | | Monterey sand | - | - | - | - |

* values inferred from the context - values not given in the text

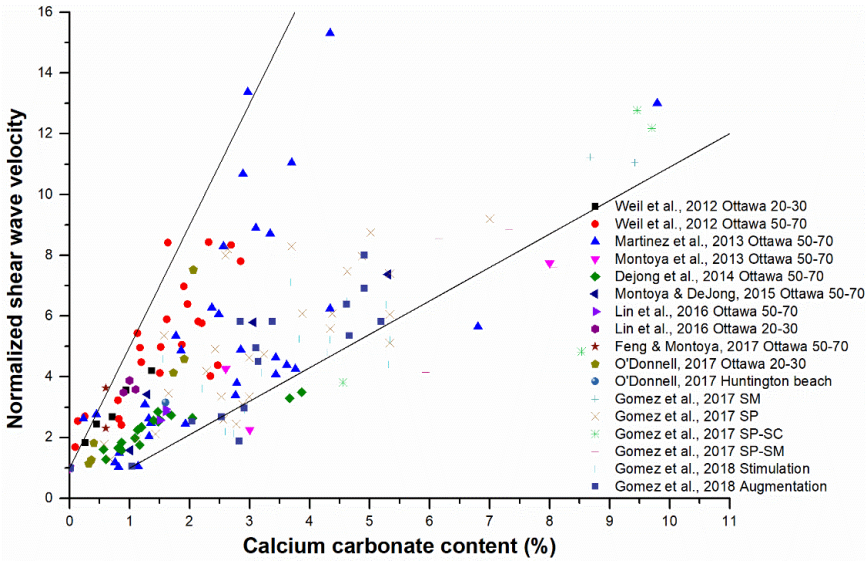


Fig. 3 Normalized shear wave velocity as a function of calcium carbonate content from various articles

origin of these large differences. Obviously, the strength of the soil, for a given percentage of carbonate, will be higher if the crystals are located at the contact points between particles rather than on the surface of particles but nothing, in the papers, confirms this assumption. The different protocols used, the activity of bacteria, etc. may explain the large scatter of the results. In the range of calcium carbonate percentages used in practice (i.e., smaller than 5%), the curve shows that one can expect an unconfined compression strength comprised between 0 and 1.4 MPa (e.g. for 5%, 0.7 MPa ± 0.7 MPa).

### *2.2 Shear wave velocity*

Shear waves are very small-strain elastic waves propagating in materials, in which particle displacement is

perpendicular to the direction of propagation (Dejong *et al.* 2010). The shear wave velocity $V_s$ is an effective stress parameter that can be a direct measure of the stiffness of the material (Hussien and Karray 2016). In an isotropic soil, it is related to the shear modulus $G_{max}$ (which is defined as the ratio of shear stress to shear strain) by the following relation: $G_{max} = \rho V_s^2$, where $\rho$ is the soil density. The measurement of $V_s$ is a nondestructive and real-time method, widely-used in the lab and in the field to estimate the elastic properties of soil (Ahmadi and Akbari Paydar 2014). For example, it can be used, together with the National Earthquake Hazards Reduction Program (NEHRP) site classification, to predict the susceptibility of a soil to liquefaction (Weil *et al.* 2012). Measurement of shear wave velocity is carried out by conventional experiments using resonant column, bender elements or piezoelectric ring-actuators in the laboratory, and by seismic cone penetration tests (SCPT) and surface waves in-situ (Weil *et al.* 2012; Hussien and Karray 2016). $V_s$ is mainly influenced by particle-particle stiffness that depends on cementation level as well as soil density, confining pressure and degree of saturation. It can be used to monitor the cementation process during MICP (Martinez *et al.* 2013, Dejong *et al.* 2014, Lin *et al.* 2016) and ensure that cementation level is sufficient to satisfy engineering application requirements. Feng and Montoya (2017) compared the cyclic behavior (strains and excess pore pressures) of two specimens (with similar $CaCO_3$ content, $V_s$ = 425 and 676 m/s, respectively). The observed difference in cyclic resistance indicated that $V_s$ was a more reliable indicator of the effect of MICP treatment on mechanical behavior than the $CaCO_3$ percentage. $V_s$ measurement is also used in some studies to monitor the degradation of cementation of MICP during loading (breakage of particle-particle contacts in soil causes $V_s$ to decrease) (Montoya and Dejong 2015, Feng and Montoya 2017).

Fig. 3 shows the change in the normalized shear wave velocity, i.e., the value of $V_s$ after MICP-treatment divided by the initial $V_s$ of the untreated soil, as a function of the $CaCO_3$ content. The normalized $V_s$ values are scattered, which is caused by the various distributions of $CaCO_3$ resulting from the different used MICP protocols. Most of the points are located above the 1:1 line, meaning that every 1% of $CaCO_3$ produced can result in more than 1-fold increase in $V_s$. The points for relatively coarse sand (Ottawa 20-30) are located in the upper part of the graph. Similar results can also be derived from O'Donnell *et al.* (2017): for the same MICP treatment, the final increment of $V_s$ for Huntington beach soil (relatively fine soil) was smaller than that of Ottawa 20-30 sand. This can possibly be attributed to the fact that the coarsest sand (Ottawa 20-30 sand) has less particle-particle contacts than the finest sands (Ottawa 50-70 and Huntington beach sand), which means that it needs less $CaCO_3$ to increase the bulk properties ($V_s$ values). It should be noted that O'Donnell used denitrifying bacteria that produced gas in the pore space, and we do not know from the text whether shear wave velocities were measured before or after the saturation process in the triaxial cell, so it is not possible to know if the results are influenced by the saturation degree.

The effect of relative density on normalized shear wave velocity is not clear. Martinez *et al.* (2013) and Dejong *et al.* (2014) tested samples with relatively high relative densities (Table 1), and the points are distributed all over the graph without preference, which means that, surprisingly, relative density might be not very important for the development of $V_s$ during MICP. Concerning the effect of confining pressure, there are very few available results and it is difficult to derive a definite conclusion. In Fig. 3, the results of Lin *et al.* (2016) show that, for similar increase in $CaCO_3$ content, the increments of normalized $V_s$ are similar regardless of confining pressure (Table 1). This is perhaps due to the relatively close confining pressures they used.

There is a large scatter in the results shown in Fig. 3. According to Weil *et al.* (2012), for the same $CaCO_3$ content, the precipitation of $CaCO_3$ at the particle-particle contacts results in higher strength or stiffness increase than when $CaCO_3$ is deposited in the pore fluid or on exposed particle surfaces. Most of the results of Gomez and Dejong (2017) and Gomez *et al.* (2018) are located below the others, maybe because many $CaCO_3$ crystals precipitated on the soil surface, as shown in the SEM images of Gomez and Dejong (2017), and inhomogeneous distribution of $CaCO_3$ was observed in the tank specimens of Gomez *et al.* (2018). Their results are interesting these researchers used a different protocol by stimulating native microorganisms in the soil rather than directly injecting well-prepared bacteria solutions as in the other studies. Their results are quite helpful as a reference for practical use in-situ, because using indigenous bacteria can avoid potential ecological impacts that may result from introducing non-native bacteria species and save the cost (laboratory cultivation and transportation). There are also inefficient MICP precipitation cases, as reported in Weil *et al.* (2012), Montoya *et al.* (2013) and Feng and Montoya (2017). The inefficient cases of Weil *et al.* and Feng and Montoya might be due to different precipitation patterns or distributions of $CaCO_3$. For Montoya *et al.* (2013), the plug formed by uneven MICP treatment in the outlet of the sample led to inflated $CaCO_3$ content but low shear wave velocity. Some points of Martinez *et al.* (2013) in the lower and right part of the figure were also due to a plug of calcium carbonate near the inlet of the cell.

In some studies, linear relationships between $V_s$ and $CaCO_3$ content were established (Al Qabany *et al.* 2011, Weil *et al.* 2012, Martinez *et al.* 2013, Dejong *et al.* 2014), but with such limitations that these relations can only be used in relation with their own MICP process. In fact, it is quite hard but helpful to give a relationship that can be generally used. As Weil *et al.* (2012) suggested, parameters reflecting soil characteristics (size, particle-particle contact stress) and possible spatial distribution of $CaCO_3$ can help establish an advanced relationship.

### *2.3 Oedometric consolidation tests*

Oedometric tests allow to measure the compressibility of a soil under nil transversal strain conditions. When the change in void ratio is plotted as a function of the axial

stress (in logarithmic scale) on a loading path, the oedometric curve features two segments of straight lines: for stresses lower than the preconsolidation stress, the behavior is reversible and the slope of the line is called the "swelling coefficient $C_s$"; for stresses larger than the preconsolidation stress, the behavior is irreversible and the slope is called the "compressibility coefficient $C_c$".

To the authors' knowledge, there are few available studies using oedometric tests. Results of Cardoso *et al.* (2016) (using uniformly graded 0.075-0.425 mm sand) showed limited increase in swelling coefficient $C_s$ (0.009-0.013) and nearly unchanged compressibility coefficient $C_c$ (0.057-0.058). Cardoso *et al.* explained that the changes in the elastic behavior of the MICP-treated soil could be attributed to bond breakage during loading. These non-obvious effects were owning to the treatment process under nil vertical stress. Results of Cardoso *et al.* (2018) showed that elastoplastic coefficient $C_c$ increased and elastic value $C_s$ remained unchanged, either when using only sand (uniformly graded 0.4-2 mm sand) or the same sand mixed with 26 % kaolin. Values of $C_c$ for the sand mixed with distilled water or MICP-treated were 0.044 and 0.089, respectively. Values of $C_c$ for the sand-kaolin mixtures mixed with distilled water, cementation solution only, and MICP-treated were 0.075, 0.145 and 0.127, respectively. The decrease of compressibility of MICP-treated samples was possibly due to the small amount of $CaCO_3$ and bond breakage during loading (Cardoso *et al.* 2016, 2018). Unfortunately, the $CaCO_3$ contents of the specimens were not provided. For sand with kaolin, osmotic consolidation (i.e., sensitivity to pH and ionic strength of clay) played a more significant role than MICP treatment in increasing $C_s$. For future study of MICP-treated sand with clay, chemical effects should be taken into consideration.

In the confined compression tests of Lin *et al.* 2016 on Ottawa 50-70 sand, using triaxial system, $C_c$ was equal to 0.024 for untreated specimen, and 0.009 for MICP-treated specimen (2.6 % $CaCO_3$). In the case of the tests on Ottawa 20-30 sand, $C_c$ was equal to 0.019 for untreated specimen, and 0.009 for MICP-treated specimen (1.6 % $CaCO_3$). MICP-treated specimens featured a lower compressibility compared to untreated soil. As expected, compressibility decreases with increasing cementation level. The same conclusion was reached by Xiao *et al.* (2021) who also observed that, in the case of Fujian silica sands ($C_u$=1-10, $d_{50}$=0.4-0.95 mm, $d_{max}$=1 mm), cementation breaking occurred at about 30 kPa while particle breaking occurred around 3 MPa. The particle breaking stress can be lower in the case of calcareous sands.

### 2.4 Triaxial tests

#### 2.4.1 Consolidated drained tests

Isotropically Consolidated Drained (ICD) triaxial tests are considered as one of the best ways to estimate the behavior of a granular soil and derive its constitutive law. Usually, the results of the tests are plotted in the Mohr-Coulomb coordinate system [$\sigma_n$, $\tau$] and two parameters are derived from the linear failure criterion: the friction angle $\phi$ corresponding to the slope of the failure criterion, and the intersection of the failure criterion with the vertical axis that is called cohesion ($c$). The same parameters may also be derived from the loading paths plotted in the [p, q] coordinate system. Here, the slope of the failure criterion is called $M$, which is related to $\phi$.

Analysis of the results found in the literature was carried out to highlight the change in failure criterion and maximum volumetric changes (contractancy and dilatancy) due to MICP treatment. Unfortunately, very few tests could be re-interpreted for different reasons: (i) the absence of the original stress-strain curves and volumetric strain versus axial strain curves in the papers; in many papers, the only available results are the failure criteria, but often without information about what these criteria represent (peak values or residual values), (ii) the fact that several investigators performed tests under a single confining stress (e.g. Waller, 2011), (iii) the use of unfounded assumptions to interpret the results of the tests; for instance, some researchers (e.g. Gao *et al.* 2019) assumed that the failure criterion was represented by the line that links the origin to the (maximum) deviator stress (i.e., that the soil cohesion was nil, whatever the MICP treatment), which results in very high and unrealistic values of the friction angle. In addition, the conditions of saturation of the samples are seldom indicated in the papers. For all these reasons, the analysis of the effect of MICP treatment on the failure criterion is very difficult to carry out seriously and is based only on the results of a small number of research groups. The results are plotted in Figs. 4(a)-4(l) for 6 soils and various treatments. The median diameter of the grains ($d_{50}$) and the uniformity coefficient of the soil ($C_u$) are indicated in the captions. In some cases where several treatments were done (e.g., Feng and Montoya 2016), one treatment corresponds to a range of several percentages of $CaCO_3$ deposited in the soil, for instance for highly cemented specimens, to percentages ranging from 4.3-5.3, which may introduce some scatter in the results. Note that the results of Li (2015) (Figs. 4(c)-(d)) were obtained for two confining stresses only, which is hardly enough to plot a reliable failure criterion. It must be pointed out that, in all of the cases, the analysis of the effect of MICP treatment on the Critical State Line (CSL) could not be carried out due to the lack or uncertainty of data.

As observed in soils cemented with cement or lime, Fig. 4(a)-4(l) shows that MICP-cementation has little or no effect on residual values: when the bonds formed by the cement between the particles are broken, the behavior is that of the original (uncemented) material. In general, when there is a difference between the residual values of treated and untreated soils, this difference is due to the fact that the tests were stopped too soon, before reaching the real residual value. Therefore, the only observed effect of MICP is an increase in the peak properties.

Based on the results of the different researchers, the cohesion of the treated specimens was plotted in Fig. 5 as a function of formed calcite content. As observed in the case of UCS, the cohesions vary largely from one test to another, and the regression coefficient $R^2$ is low (0.69). However, these results show a definite increase in cohesion with calcite content, reaching several hundreds of kPa in the results of Terzis and Laloui (2019) and Gowtaman (2021)

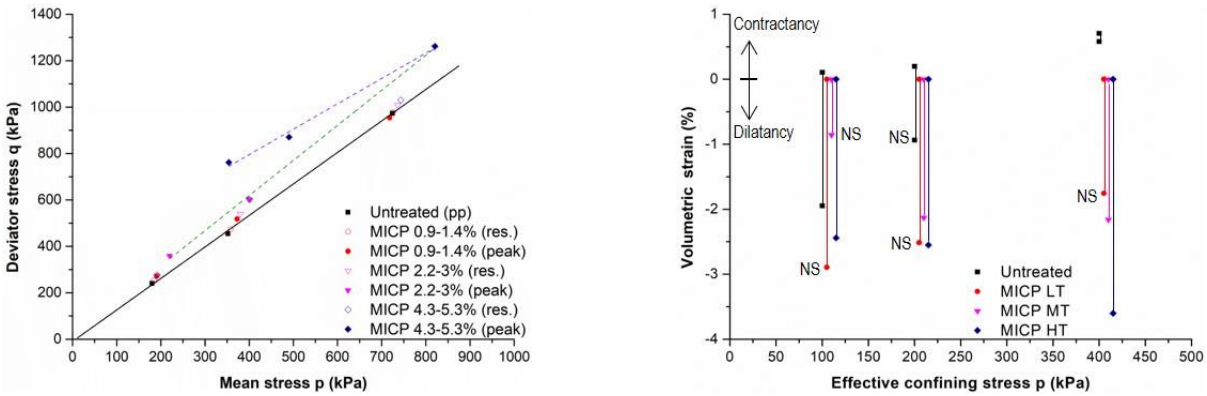


(a) & (b) Feng and Montoya (2016) on fine sand ($d_{50}$ = 0.22 mm, $C_u$ = 1.4)

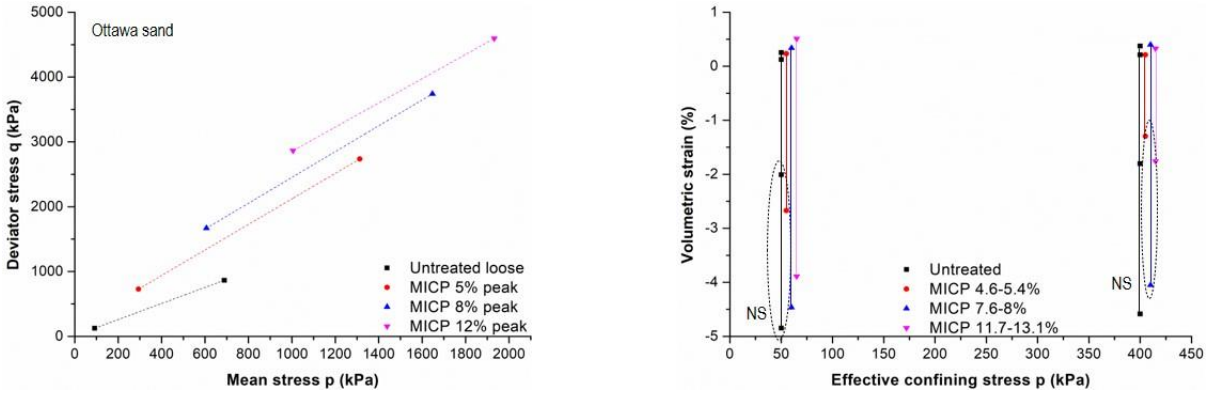


(c) & (d) Li (2015) on medium Ottawa sand ($d_{50}$ = 0.4 mm, $C_u$ = 1.5)

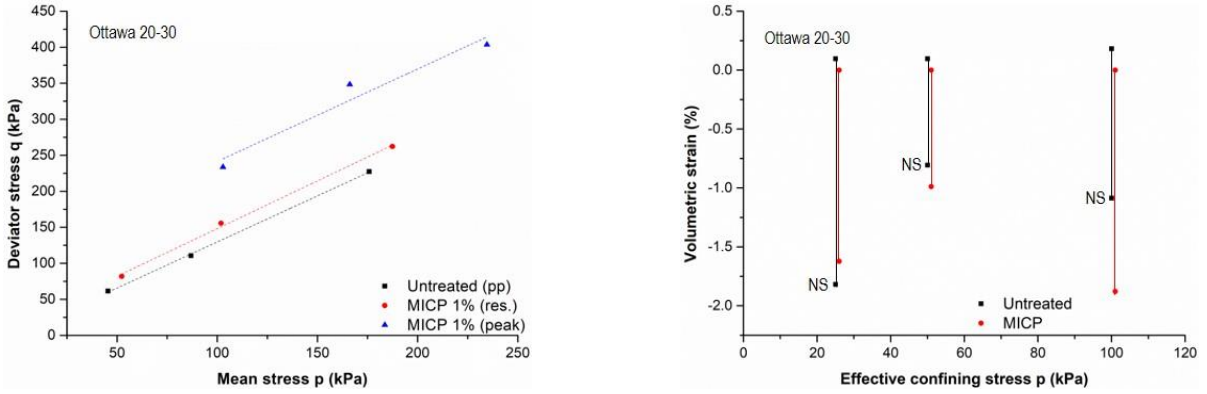


(e) & (f) Lin (2016) on Ottawa 20-30 sand ($d_{50}$ = 0.71 mm, $C_u$ = 1.2)

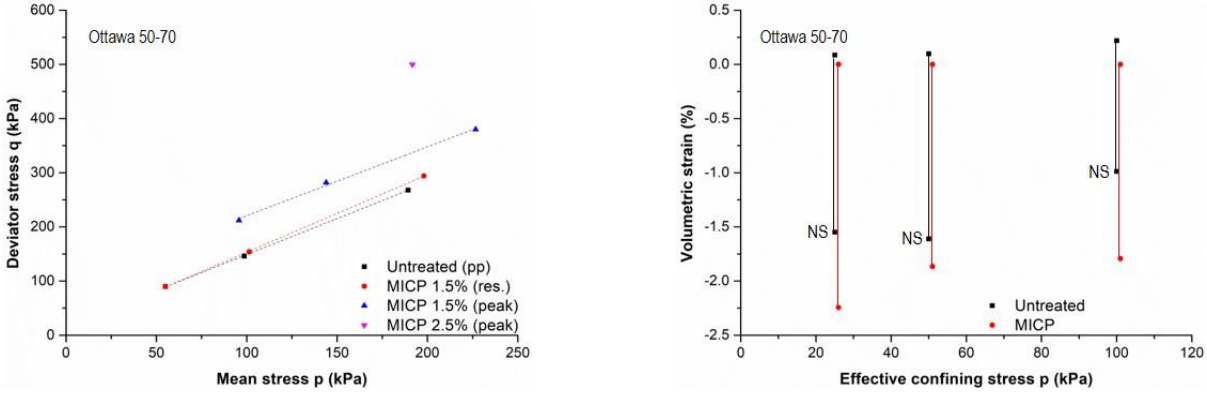


(g) & (h) Lin (2016) on Ottawa 50-70 sand ($d_{50}$ = 0.33 mm, $C_u$ = 1.2)

Fig. 4 Reinterpretation of the results of the literature [pp: perfect plasticity, peak: maximum strength; res.: residual strength after peak]

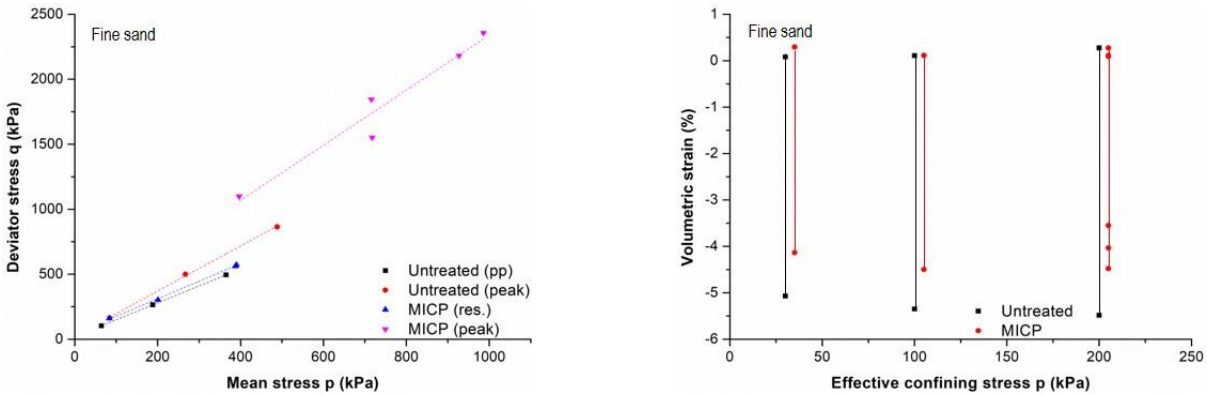


(i) & (j) Terzis and Laloui (2019) on fine sand ($d_{50}$ = 0.19 mm, $C_u$ = 2.1)

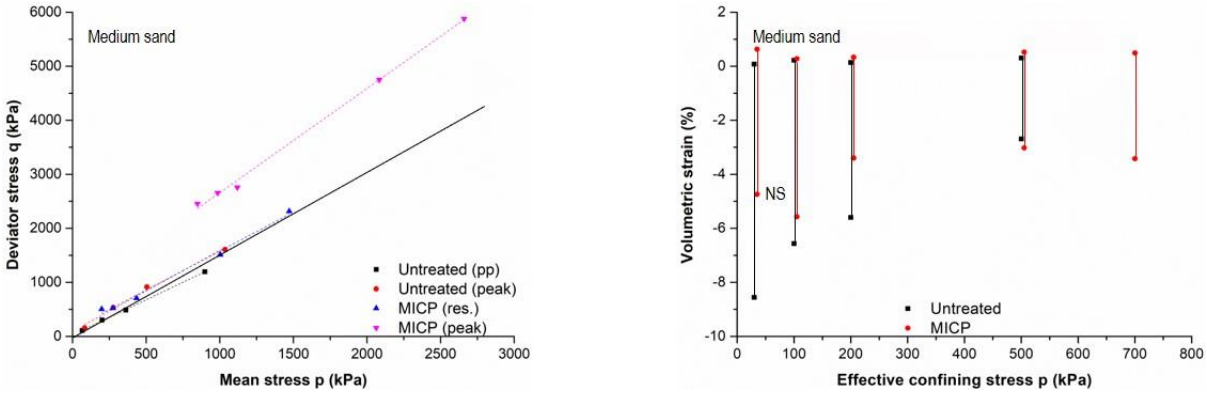


(k) & (l) Terzis and Laloui (2019) on medium sand ($d_{50}$ = 0.39 mm, $C_u$ = 1.6)

Fig. 4 Continued

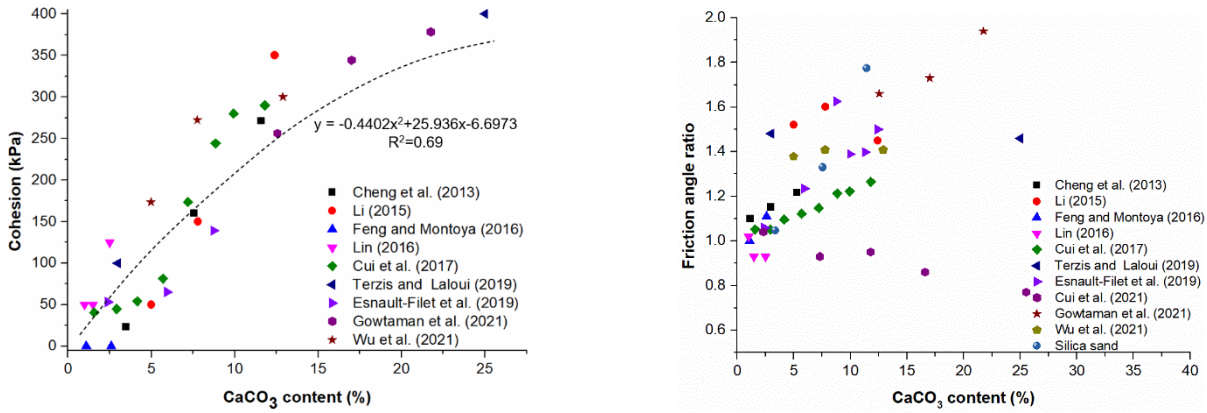


(a) (b)

Fig. 5 Synthesis of CD triaxial tests: (a) cohesion and (b) friction angle ratio as a function of formed $CaCO_3$ content

for $CaCO_3$ contents larger than 20%. The same analysis was attempted in the case of friction angles but the scatter is much more important and the regression coefficient $R^2$ does not exceed 0.2, meaning that there is no correlation between the two parameters. In fact, a few researchers (e.g. Feng and Montoya 2016, Cui *et al.* 2021) observed a decrease in friction angle when the calcite content increased, while most others highlighted an increase in friction angle, for instance, from 33-35° to 49-51° for Terzis and Laloui (2019), from 40° to 50° for Esnault-Filet *et al.* (2019) in the case of Fontainebleau sand ($d_{50}$ = 0.21 mm, $C_u$ = 1.5). Interesting results were published by Montoya and Dejong (2015) who carried out drained tests on Ottawa 50-70 sand at a confining stress of 100 kPa on different loading paths (axial compression, constant p and radial extension). Unfortunately, the results of the tests are too scattered to derive a definite conclusion on the effect of stress path.

Another effect of MICP treatment that is often cited in the papers is the large dilative behavior of MICP-treated soils. It should be mentioned here that this parameter is often difficult to estimate precisely as, in most of the papers, the tests are carried out to relatively small maximum axial strains (12 to 15%) and without anti-friction devices, which often does not allow dilation to fully develop (this is

noted NS in the figures). In addition, this parameter is highly dependent on relative density, whose value is not always mentioned in the papers. Figs. 4(b)-4(l) show the maximum contractancy and maximum dilatancy for the different tests analyzed here as a function of the effective confining stress. In practically all the tests, the contractive behavior is similar between untreated and treated specimens. Concerning the dilative behavior, the results are rather dispersed and depend on the level of cementation and confining stress. Globally, dilatancy does not seem to decrease when the confining stress increases, nor to increase with the level of cementation. For instance, in the results of Lin (2016) on Ottawa 50-70 sand, or Terzis and Laloui (2019) on fine sand, the dilation strains are of the same order of magnitude for untreated and treated specimens, even lower for treated specimens in the second case. In the other studies, the values may be close for some confining stresses, and different for others. It should be pointed out also that, in the case of heavily bio-cemented soils, failure occurring at the peak is not homogeneous and features a failure surface, making it more difficult to measure correctly the volumetric strains. Therefore, concerning the aspect of dilative behavior, the conclusion is not clear and more tests are necessary.

#### *2.4.2 Consolidated undrained monotonic triaxial tests*

The behavior of MICP treated specimens on *Isotropically Consolidated Undrained* (ICU) triaxial paths can be derived from that of the samples on ICD triaxial tests: the changes in volumetric strains will result in changes in pore pressure, which will affect the strength of the soil through the effect of the effective stresses. The few results available in the literature are often difficult to re-interpret because of a lack of precise data. Montoya and Dejong (2015) performed tests on untreated and treated samples of Ottawa 50-70 sand ($d_{50}$ = 0.22 mm, $C_u$ = 1.4, $D_R$ ≅ 40%) under one confining stress. To interpret their results, they considered that the cohesion was unchanged by the treatment and that the increase in strength was due to an increase in the peak friction angle. However, in the case of CU tests, the failure criterion can also be defined with reasonable accuracy by the stress path when the sample reaches perfect plasticity, as shown for instance by O'Donnell *et al.* (2017).

Re-interpretation of the results of Montoya and Dejong (2015), using this method, led to the data of Table 2 that show an increase in cohesion with the treatment, and the invariance of the friction angle. O'Donnell *et al.* (2017) carried out tests on undisturbed and MICP-treated (1% $CaCO_3$) Ottawa 20-30 sand ($d_{50}$ = 0.7 mm, $C_u$ = 1.2, $D_R$ = 45%) and obtained the same friction angle and an increase in cohesion of 37 kPa. Hataf and Jamali (2018) studied the effect of MICP treatment on binary mixtures of sand ($d_{50}$ = 1.3 mm, $C_u$ = 2.4) and clay (100% < 75 µm, $d_{50}$ = 6 µm, $C_u$ > 10). They concluded that the treatment resulted in no change of friction angle and cohesion for clay contents larger than 30%, and a large increase in cohesion for clay contents of 10 and 20%. However, these results are difficult to interpret as the untreated remolded clay featured an unexpected cohesion of nearly 50 kPa. Globally, the conclusions of these studies seem qualitatively consistent with those of the CD triaxial tests, but there is a dire need for more results to confirm the conclusions.

Table 2 Reinterpretation of the results of Montoya & DeJong (2015)

| MICP treatment: $CaCO_3$ content | | 0 | 1% | - | 1.3% | 3.1% | 5.3% |
|---|---|---|---|---|---|---|---|
| $V_s$ (m/s) | | 190 | 300 | 450 | 650 | 1100 | 1400 |
| Interpretation of Montoya and Dejong (2015) | $c$ (kPa) | 0 | 0 | 0 | 0 | 0 | 0 |
| | $\phi$ (°) | 33 | 33.6 | 37.4 | 39.2 | 41.5 | 43.7 |
| Re-interpretation of the results | $c$ (kPa) | 0 | 10 | 35 | 55 | 85 | 95 |
| | $\phi$ (°) | 31.7 | 30.3 | 31.1 | 31.1 | 31.1 | 31.1 |

- value not given in the text

#### *2.4.3 Consolidated undrained cyclic triaxial tests*

Undrained cyclic triaxial tests on saturated MICP treated soils, in which the samples are subjected to compression-extension solicitations under controlled conditions of stress deviator, all show the same trend of result:

• A slower increase in pore pressure and axial strain in treated samples, compared to untreated soils.

• A larger number of cycles necessary to reach liquefaction for the same value of the cyclic stress ratio (CSR), which is equal to the ratio of the half cyclic deviator stress to the effective consolidation stress (i.e., $q_c/2\ \sigma'_3$).

As a consequence, the classical liquefaction curves that represent the relation between the CSR and the number of cycles leading to liquefaction ($N_L$) are shifted to the right or upward (i.e., to higher number of cycles or cyclic deviator stress) when the soil is cemented by MICP, all the more so as the $CaCO_3$ content is higher. Of course, these curves depend on other factors like the type and grading of the soil, the relative density of the samples, etc. The latter is especially important as the mass of formed $CaCO_3$ is taken into account in the dry mass of the sample, which leads to an increase in its relative density. For example, in a standard sand (e.g. $e_{max}$=0.84; $e_{min}$=0.55) the formation of 9% $CaCO_3$ increases the relative density from 30% to more than 80%, and the initially "loose" sand may become finally a "dense" sand.

Riveros and Sadrekarimi (2020) concluded from their tests on fine Fraser river sand that MICP-treatment led to a change of the failure mechanism, from liquefaction failure in the untreated sand to cyclic mobility in the MICP-treated samples. To try to compare the results obtained by different researchers in the literature, the vertical shift of the liquefaction curves was plotted in Fig. 6 as the normalized CSR ($CSR_{norm}$), i.e., the ratio of the CSR for the treated soil to that for the untreated soil for two numbers of cycles: (a) for $N_L$ = 10 cycles, and (b) for $N_L$ = 100 cycles. Several conclusions can be drawn from Fig. 6:

• There is a large scatter in the results, even if the relative densities are similar, so that it is difficult to draw a quantitative conclusion;

• The effect of MICP is more important when the initial relative density of the soil is lower;

• For the same initial relative density, the normalized

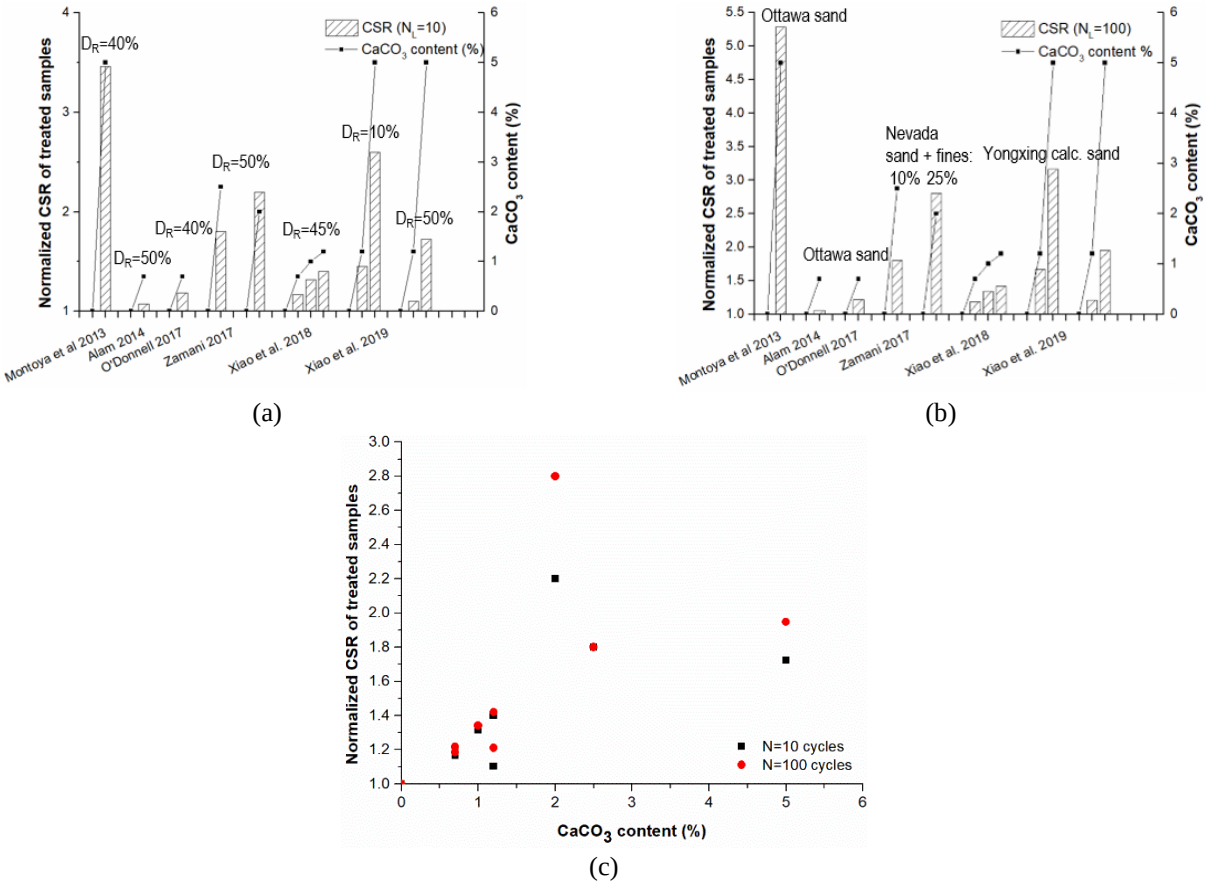


Fig. 6 Ratio of CSR of treated soils to CSR of untreated soils and corresponding $CaCO_3$ contents (a) for a number of 10 cycles leading to liquefaction, (b) for a number of 100 cycles leading to liquefaction and (c) as a function of the $CaCO_3$ percentage for relative densities ranging from 40-50%

$CSR_{norm}$ increases with the $CaCO_3$ content (Fig. 6(c)). For instance, for $N_L$ = 10 cycles: for a very light treatment (0.7% of $CaCO_3$), the effect of the treatment is hardly visible ($CSR_{norm} \cong$ 1.1 to 1.2); for a light treatment (1.2% of $CaCO_3$), $CSR_{norm}$ is equal to 1.5; for a medium treatment (2.5% of $CaCO_3$), $CSR_{norm}$ is equal to 2.5; and for heavily treated specimens (5% of $CaCO_3$), the normalized CSR reach 2.7 to 3.5.

Of course, all these conclusions are based on a very small number of results and should be controlled and confirmed by additional tests, especially as the information about the materials, the tests, the $CaCO_3$ content, etc. is often incomplete, sometimes missing.

Porcino (2011) performed simple shear tests on untreated and MICP-treated specimens of sand and observed that, for untreated samples, the pressure build-up was similar to that obtained during triaxial tests whereas, for treated specimens, the pressure build-up was much slower in the simple shear tests than in the triaxial tests. Lee *et al.* (2020), using a dynamic shear test device with Ottawa F65 sand, found that the presence of even low levels of cementation could significantly alter the cyclic resistance of sands subjected to CSRs of 0.1 and 0.2 with approximately one order of magnitude increase in the number of cycles required to trigger liquefaction. However, post-triggering shear strain accumulation was not significantly affected at these low levels of cementation.

### *2.5 Centrifuge tests*

As shown in the previous paragraph, MICP can effectively mitigate liquefaction by reducing excess pore pressure and deformation. Centrifuge tests on loose ($D_R$=40%) untreated and moderately MICP-treated Ottawa 50-70 sand subjected to a series of shaking events with increasing shaking amplitudes were carried out by Montoya *et al.* (2012). The level of shaking is characterized by the maximum acceleration $a_{max}$ at the base of the model. The pore pressure parameter $r_u$ that represents the ratio of the excess pore pressure to the vertical effective stress, is often used to characterize the effect of treatment on the increased resistance to liquefaction. For the results of free-field soil response, MICP-treated sample showed a marked reduction in the generation of excess pore pressure at both low ($a_{max}$ = 0.3 g) and high ($a_{max}$ = 0.7 g) levels of shaking, but a longer time was needed to dissipate the excess pore pressure due to the reduced permeability caused by $CaCO_3$ precipitation (refer to § 2.6): in the first case ($a_{max}$ = 0.3 g), $r_u$ ranged from 0.15-0.2 from depth to surface for MICP-treated samples, compared to $r_u$ = 0.4-1.0 for untreated samples whereas, in the second case ($a_{max}$ = 0.7 g), $r_u$ ranged from 0.3-0.4 from depth to surface for

MICP-treated samples, compared to $r_u$ = 0.7-1.0 for untreated samples. When untreated, the soil below the structure experienced similar generation of excess pore pressure, with values of $r_u$ = 0.25-1.0 from depth to surface at low shaking levels ($a_{max}$= 0.3 g), and $r_u$ = 0.6-1.0 from depth to surface at high shaking levels ($a_{max}$= 0.7 g). MICP-treated soil generated very little excess pore pressure at both low and high levels of shaking. Smaller deformations in the sand beneath the structure were also seen in the MICP-treated sample, with average vertical strains equal to 8.4 % at 5 m depth, and 24 % at the surface, for the untreated sample, compared to values of 2 % and 9 % for the MICP-treated sample.

In the following study of Montoya *et al.* (2013), centrifuge tests on MICP-treated samples with different cementation levels (lightly cemented with a target shear wave velocity $V_s$ = 350 m/s, moderately cemented with $V_s$ = 660 m/s, heavily cemented with $V_s$ = 1200 m/s) were conducted using the same sand and the same centrifuge model, and the results were compared to those on loose ($D_R$ = 40%) and dense ($D_R$ = 85%) untreated sands. The behavior of the loose sand obtained from centrifuge tests showed a soil-to-rock-transition with increasing cementation level. As observed by many researchers, the resistance of the dense untreated sand to dynamic loading was markedly enhanced by comparison with the loosely untreated sand, with an evidence of lower values of $r_u$. All degrees of MICP-treated samples featured a lower $r_u$ value (well below 1.0) at both shaking levels, which demonstrates the increased ability to resist dynamic loading. When subjected to a series of ground motions, at first, the trend of increments in shaking-induced settlements and their magnitudes in MICP-treated samples were similar to those of dense untreated sand. After a certain amount of degradation of cementation was achieved, the settlements of MICP-treated samples showed an increase, similarly to loosely untreated sand. But the settlement values were still smaller than those for the loose untreated sand, which indicates an improvement in resistance to cyclic loading. Darby (2019) also applied repeated shakings to centrifuge models of untreated and MICP-treated Ottawa sand (DR = 38 and 53%) with low (0.8%), moderate (1.4%) and high (2.2%) $CaCO_3$ contents. Results showed that moderately and heavily MICP-treated sand needed larger peak base accelerations (PBAs) to trigger liquefaction than untreated loose and medium sands, with values of 0.17g, 0.45g, 0.06g and 0.12g, respectively. For lightly cemented sand, the PBA to trigger liquefaction was between those of untreated loose and medium-dense sands: The higher the cementation level, the higher the PBAs to trigger liquefaction.

Interestingly, higher maximum surface accelerations values were obtained by Montoya *et al.* (2012) in MICP-treated samples compared to loosely untreated sand under high (0.7 g) shaking dynamic loading. Zhang *et al.* (2020) also found that surface accelerations of MICP-treated calcareous sand in shaking table tests were amplified. Of course, these results are related to the higher stiffness of treated soil. The undesirable higher surface motions need to be considered when applying MICP methods in-situ.

The conclusion of these tests is that MICP-treated specimens need higher accelerations to trigger liquefaction, and that the treatment can help reducing excess pore pressure and settlements, which can help them to resist cyclic loadings. The conclusions of centrifuge tests are highly consistent with those of undrained cyclic triaxial tests, but they are also based on a very small number of tests and remain mostly qualitative.

## 3. Hydraulic properties of MICP-treated soils

Permeability ($k$) is a crucial geotechnical parameter to describe fluid flow in soil. It reflects how easily the fluid is able to pass through the pores. In soil columns, permeability is usually measured by constant head tests (for coarse grained soil) or falling head tests (for fine grained soil). Fig. 7 shows the change in normalized permeability, i.e., the ratio of permeability after MICP treatment to its initial value before treatment, as a function of the carbonate content deposited in the soil, and Table 3 indicates the parameters of the permeability tests in the literature.

After MICP treatment, the permeability of the soil is usually changed. In most cases, permeability is reduced by less than 1 order to 2 orders of magnitude. For example, in the study of Yasuhara *et al.* (2012), the $k$ values dropped from $4 \times 10^{-4}$ m/s to $10^{-6}$ - $10^{-7}$ m/s. The treatments of Eryürük *et al.* (2015) reduced $k$ from $8.4 \times 10^{-3}$ - $4.1 \times 10^{-5}$ m/s to $9.9 \times 10^{-6}$ - $2.1 \times 10^{-8}$ m/s. The results of Wen *et al.* (2019) indicated that the permeability was reduced from $1.4 \times 10^{-3}$ m/s to $1 \times 10^{-5}$ m/s after four treatment injections. A marked reduction was seen during the first treatment, followed by gradual reduction. On the other hand, the $k$ values experienced only one, or less than one, order of reduction (from $10^{-7}$ to $10^{-8}$ m/s) in the study of Safavizadeh *et al.* (2017). In some cases, permeability stayed almost unchanged. Whiffin (2004) observed a minor decrease of 2-14 % of the porosity and almost unchanged permeability. Jiang and Soga (2017) found that MICP-treated sand-gravel mixed soil showed a limited reduction of $k$ after treatment, the increase in cementation concentration having only a slight effect on the reduction of $k$.

As reported in El-Latief *et al.* (2015) suspension-based fine grouts (cement grouts, cement-bentonite grouts and clay grouts) decrease the permeability of about 3-5 orders of magnitude, and chemical grouts (acrylamide grout, NMA grout) reduce permeability of about 6-8 orders of magnitude. An advantage of MICP-treatment is that soils can retain a relatively high permeability compared to other grouting methods. For example, higher permeability can reduce the failure risk of a foundation (such as that of hydraulic structures) by lowering the uplift of pore water pressure, which in turn lowers the cost of construction and installation of a drainage system in-situ (Cheng *et al.* 2013). And it also permits additional treatment in terms of engineering requirements.

In Fig. 7, the general trend is that permeability decreases as the $CaCO_3$ content increases. Loss of permeability in MICP-treated soil is caused by (i) reduction of porosity, due to the occupation of the space by forming $CaCO_3$ crystals (Martinez *et al.* 2013), (ii) plugging by the forming crystals

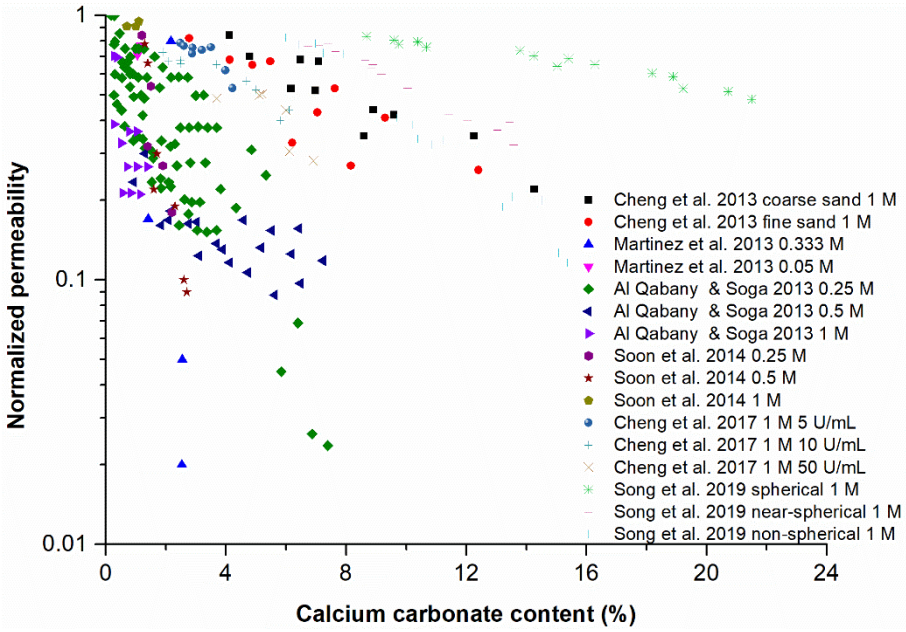


Fig. 7 Normalized permeability as a function of calcium carbonate content from various articles

Table 3 Parameters of permeability tests in the literature

| Reference | Sand | $d_{50}$ (mm) | $C_u$ | $D_R$ (%) | Porosity | Bacteria |
|---|---|---|---|---|---|---|
| (Cheng *et al.* 2013) | Fine sand | 0.205 | 1.57 | - | 0.39 | *Bacillus sphaericus* |
| | Coarse sand | 0.7 | 1.39 | | | |
| (Martinez *et al.* 2013) | Ottawa 50-70 | 0.21 | 1.4 | 78-100 | 0.34-0.38 | *S. pasteurii* |
| (Al Qabany and Soga 2013) | Grade D silica sand | 0.165 | - | 20-100 | 0.585-0.907 | *S. pasteurii* |
| (Soon *et al.* 2014) | Tropical residual soil (silt) | <0.05 | - | 90 | - | *Bacillus megaterium* |
| (Cheng *et al.* 2017) | SP | | 1.65 | 95 | 0.4915 | *Bacillus sphaericus* |
| (Song *et al.* 2019) | Artificial silica<br>Intact Ottawa<br>Crushed Ottawa | *0.21 | - | - | 0.385-0.401 | *S. pasteurii* |

* values inferred from the context - values not given in the text

in pore space or pore throats (Stocks-Fischer *et al.* 1999), (iii) bio-clogging by the biomass or related metabolic products (Ivanov and Chu 2008, Al Qabany and Soga 2013, Farah *et al.* 2016). These different causes are very difficult to discriminate in the test results. The reduction of porosity is seldom measured or mentioned in the papers. In Fig. 7, the points are very scattered and, for the same calcium carbonate content, there are large differences in the degree of reduction. This phenomenon is caused by the initial pore characteristics of the soil and precipitation patterns of $CaCO_3$ in the pore spaces due to the different treatment protocols. Al Qabany and Soga (2013) studied the effect of the concentration of the cementation solution on the reduction of permeability. At high concentrations (1M), permeability experienced a sharp drop once the $CaCO_3$ started to precipitate because it produced large crystals that plugged locally the samples. At low concentrations (0.25 M), permeability declined more gradually and the points were more scattered. In that case, the deposition of $CaCO_3$ crystals was more progressive and homogenous, and the decrease in permeability was negligible (Dejong *et al.* 2010). Concerning the effect of relative density, the normalized permeability decreased faster in denser soils ($D_R$ > 70%) than in looser soils ($D_R$ < 60%) (Al Qabany and Soga 2013). In MICP-treated soils with relative densities of 85, 90 and 95%, the normalized permeability was reduced to 0.46, 0.39, 0.26, respectively (Soon *et al.* 2013). But in Fig. 7, we cannot conclude on the effect of relative density, because of the difference in the MICP treatments. Regarding the influence of particle morphology (Song *et al.* 2019), spherical particles led to larger $CaCO_3$ contents and lower permeability reduction than non-spherical and angular particles after the same MICP treatment. In the test on spherical particles, $CaCO_3$ crystals distributed uniformly and were generated continuously on the particle surface probably because of the even adhesion of bacteria. And the reduction of permeability caused by occupation of $CaCO_3$ was not obvious. For non-spherical and angular particles, $CaCO_3$ crystals were located only on some parts of soil surface due to the roughness of soil particles. These $CaCO_3$

crystals progressively occupied slim slot-shaped pore spaces formed by irregular particles, thus decreasing permeability.

## 4. Microscopic studies

In addition to these relatively macro-scale studies, it is vital to understand more about the molecular-level chemical and biological processes (Li *et al.* 2017, Wang *et al.* 2017), in order to improve $CaCO_3$ repartition in the soil and to apply this technique to real works with various requirements. Common techniques used in various references of MICP studies include scanning electron microscopy (SEM) (Dejong *et al.* 2006, van Paassen 2009, Cheng *et al.* 2013, Soon *et al.* 2013, Choi *et al.* 2017, Simatupang and Okamura 2017, Liang *et al.* 2019, Choi *et al.* 2019), X-ray diffraction (XRD) (Sarda *et al.* 2009, Ghosh *et al.* 2019, Omoregie *et al.* 2019), Fourier-transform infrared (FT-IR) spectroscopy (Dhami *et al.* 2013, Cardoso *et al.* 2018), confocal and Raman spectroscopy (Nehrke and Nouet 2011, Connolly *et al.* 2013, Dhami *et al.* 2013), μ-CT (Dadda *et al.* 2017, Terzis and Laloui 2019), etc.

Evidence obtained from microscopic studies shows that bacteria serve as nucleation sites (Gat *et al.* 2014, Ghosh *et al.* 2019) and influence the $CaCO_3$ crystals formation. Dhami *et al.* (2013) shed light on the process of bacteria providing nucleation sites for $CaCO_3$ precipitation by capturing bacterial imprints on the surface of $CaCO_3$ crystals. Results of Ghosh *et al.* (2019) gave direct evidence that nanometer-sized $CaCO_3$ crystals deposited on the cell surface of *S. pasteurii*. They clarified the nucleation sites provided by bacteria and the likely nucleation routes using field emission scanning electron microscopy (FESEM) with Energy Dispersive X-Ray Spectroscopy (EDS), and high resolution transmission electron microscopy (TEM). Using XRD tests, van Paassen *et al.* (2009) concluded that vaterite and calcite are the dominant crystals at high and low urea hydrolysis rates, respectively.

Metabolic products secreted by bacteria also affect precipitation, e.g. by trapping calcium ions or as a result of specific proteins that influence precipitation (Kawaguchi and Decho 2002). Schultze-Lam *et al.* (1992) showed that the proteinaceous S-layer (part of the cell envelope composed by proteins) plays a part in the mineralization process. Ercole *et al.* (2012) found that both exopolysaccharides (EPS, natural high-molecular-weight polymers composed of sugar residues that are secreted by microorganisms) and capsular polysaccharides (CPS, polysaccharides layers that are part of the outer envelope of a bacterial cell) isolated from different calcifying bacteria could take part in the precipitation process by serving as nucleation sites as well as playing a direct role in $CaCO_3$ formation. Dhami *et al.* (2013) concluded that EPS can specifically combine with $Ca^{2+}$ and induce $CaCO_3$ precipitation. Specific functional groups on EPS influence the extent and types of precipitation (crystals or amorphous organominerals) (Decho 2010). Nevertheless, there is still much unknown about the precise role of the S-layer and EPS in the process of MICP. Knowledge about these mechanisms could be quite interesting to optimize the use of bacteria.

Microscopic images (e.g. SEM with EDS) contributed to the visualization of microstructures of MICP treated soil (i.e., distributions of $CaCO_3$ and the determination of the characteristics of $CaCO_3$ crystals), which are quite important to explain the differences in macroscopic engineering properties. For example, Cheng *et al.* (2013) presented images of MICP-treated sand at 100% and 20% degree of saturation. In the images of saturated samples, $CaCO_3$ crystals were distributed not only at particle contacts, but also on particle surface and in pore fluids. By contrast, at 20% of saturation, $CaCO_3$ mainly precipitated at particle contacts, which resulted in relatively higher UCS values and lower $CaCO_3$ contents. Soon *et al.* (2014) proved that the $CaCO_3$ produced by MICP formed on the soil particles as well as at particle contacts, and highlighted the bonds between soil particles in SEM images. Images of Lin *et al.* (2016) showed that $CaCO_3$ crystals contributed to contact cementing and matrix supporting between soil particles, which helped increase strength and stiffness in MICP-treated soils.

Characteristics of $CaCO_3$ crystals are important for improving engineering properties. Dadda *et al.* (2017) used synchrotron X-ray tomography combined with computed 3D images to study the microstructure (volume fraction and specific area of $CaCO_3$) and physical properties (permeability, effective diffusion) of MICP-treated soil. They concluded that the average thickness of the $CaCO_3$e layer was 6-7 μm. Their 3D images also showed that the specific surface area increases slightly when the volume fraction of $CaCO_3$ is less than 10%, and it decreases slightly when the $CaCO_3$ volume is larger than 10% owning to the new created particle contacts. Wang *et al.* (2019) and Marzin *et al.* (2020) observed the whole process of MICP and the evolution of $CaCO_3$ by using a transparent microfluidic chip combined with an optical microscope. Terzis and Laloui (2019) used time-lapse video microscopy and X-ray micro-computed tomography (μ-CT) combined with 3D volume reconstruction to characterize qualitatively the number, sizes, orientations and purity of $CaCO_3$. They found that a medium-grained sand gained larger $CaCO_3$ crystals and more homogeneous distribution of precipitations compared to the fine-grained Itterbeck sand. Another crucial finding is that the average mass of bonds does not necessarily yield the expected mechanical response, because the mechanical behaviour is also related to the intrinsic properties of the soils and the fabric of bio-cemented soil.

## 5. Conclusions

Based on the above analysis, the following conclusions can be drawn:

• UCS increases with increasing $CaCO_3$ content. In the range of calcium carbonate percentages used in practice (i.e. smaller than 5%), the results show that one can expect an UCS up to 1.4 MPa (e.g., for 5%, 0.7 MPa ± 0.7 MPa). For a given $CaCO_3$ percentage, the densest specimens, and the specimens with the more widespread grain size distribution, feature the highest UCS.

• When subjected to monotonic loadings, MICP-treated soils show an increase in the peak properties, an indefinite increase in friction angle and a large increase in cohesion with the $CaCO_3$ content. Concerning the dilative behavior, the results are rather dispersed and depend on the level of cementation and confining stress.

• When subjected to cyclic/dynamic loadings (triaxial, simple shear or centrifuge tests), marked enhancement can be seen in lowering the pore pressure generation, reducing the strains, decreasing peak base acceleration (to trigger liquefaction) and number of cycles to reach liquefaction in MICP-treated soil. The effect of MICP is more important for 10 cycles than for 100 cycles, and when the initial relative density of the soil is lower. For the same initial relative density, the normalized $CSR_{norm}$ increases with the $CaCO_3$ content. MICP-treated soils feature a progressive soil to rock transition for an increasing cementation level.

• Similarly, the shear wave velocity $V_s$ increases with increasing cementation level ($CaCO_3$ content) but, as for the other properties, this increase highly depends on where $CaCO_3$ crystals precipitate: if precipitation takes place at particle-particle contacts, the increase in $V_s$ is important. Growing $CaCO_3$ crystals on the soil particle surface is less efficient but may eventually enhance properties as well. In most cases, for every 1% $CaCO_3$ precipitated, more than 1-fold $V_s$ increment can be expected.

• In most cases, the drop in permeability due to MICP treatment remains limited to less than 1 to 3 orders of magnitude. Normalized permeability decreases with increasing $CaCO_3$ content. The decrease is larger when the cementation solution is more concentrated, and in more angular soils.

• The data of the literature (normalized UCS, $V_s$, and especially $k$ values) are very scattered, which is caused by using various materials (soils, strains of bacteria) and MICP protocols. Incorporating parameters that reflect soil characteristics (e.g. size, particle-particle contact), possible spatial distribution of $CaCO_3$, etc., could help establish advanced relationships between $CaCO_3$ content and $UCS/V_s/k$.

• The formation of calcium carbonate results in an increase in the dry density of the samples that may play a major part in the improvement of the soil properties, such as peak maximum deviator, resistance to liquefaction, etc. Many researchers have pointed out that the enhancement of soil properties by MICP cementation was equivalent to an increase in density, but it is not clear whether they speak of the real density increase or of the bonding of particles. This important phenomenon must be taken into account in the analyses.

• Though abundant conclusions can be drawn, there is still much work left for further studies. The previous conclusions are based on too few tests and the data of the tests are often partial or missing. This technique still needs to progress in the way of lowering cost, maximizing efficiency and adapting to goals. A few suggestions for future studies are listed below,

• MICP-treatment of soils with different compositions: Most of the existing studies use quartz sands. Because the soils to be used in-situ during construction are imposed, the studies should include different soils.

• The grain size range and grading of effective MICP treatment considering in-situ injection: The lower boundary size of grains (in order not to inhibit the transport of bacteria in the pore space) was discussed in (Dejong *et al.* 2010). On the other hand, most studies have been carried out on fine sands with limited size range (usually less than 1 mm), as shown in Fig. 2(b), Table 1 and Table 3. Very few studies explore extended grain range and relatively larger grains that are important for engineering use.

• The optimal protocols for various soils: For different soils, the varying physical characteristics might influence the efficiency of the treatment. Thus, it is essential to establish a comprehensive protocol for the application of MICP method to various soils, which will benefit its practical use in real works.

• The performance of MICP-treated soil on various loading paths: In the literature, very few studies have been carried out on the effect of loading paths and crucial parameters such as confining pressure, cyclic frequency, waveform, overconsolidation degree, etc. In most papers, shearing results are presented whereas, in terms of real applications, various environmental loadings could be met. Hence, mechanical behavior of MICP-treated soil should be explored more thoroughly.

• The role of EPS during MICP process: Microscopic studies have shown the role of EPS during MICP process, such as helping the formation of $CaCO_3$ and taking part in crystal formation. But other effects of EPS are almost unknown. It would be quite interesting to study the precise role of EPS to understand more about the basic microscopic mechanisms to optimize the MICP technique.

## Acknowledgments

The authors would like to thank the financial support of China Scholarship Council (CSC) and the assistance of Solétanche-Bachy.

## References

Ahmadi, M.M. and Akbari Paydar, N. (2014), "Requirements for soil-specific correlation between shear wave velocity and liquefaction resistance of sands", *Soil Dyn. Earthq. Eng.*, **57**, 152-163. https://doi.org/10.1016/j.soildyn.2013.11.001.

Al Qabany, A., Mortensen, B., Martinez, B., Soga, K. and Dejong, J. (2011), "Microbial carbonate precipitation: Correlation of S-wave velocity with calcite precipitation", *Proceedings of the Geo-Frontiers 2011*, Dallas, Texas, U.S.A., March.

Al Qabany, A. and Soga, K. (2013), "Effect of chemical treatment used in MICP on engineering properties of cemented soils", *Géotechnique*, **63**, 331-339. https://doi.org/10.1680/geot.SIP13.P.022.

Bahmani, M., Noorzad, A., Hamedi, J. and Sali, F. (2017), "The role of Bacillus pasteurii on the change of parameters of sands according to temperature compresion and wind erosion resistance", *J. CleanWAS*, **1**, 1-5. https://doi.org/10.26480/jcleanwas.02.2017.01.05.

Biarez, J. and Hicher, P.Y. (1994), *Elementary Mechanics of Soil Behaviour: Saturated Remoulded Soils*, A.A. Balkema, Lisse,

The Netherlands.
Cardoso, R., Pedreira, R., Duarte, S., Monteiro, G., Borges, H. and Flores-Colen, I. (2016), *Biocementation as Rehabilitation Technique of Porous Materials*, in *New Approaches to Building Pathology and Durability*, Springer, 99-120.
Cardoso, R., Pires, I., Duarte, S.O.D and Monteiro, G.A. (2018), "Effects of clay's chemical interactions on biocementation", *Appl. Clay Sci.*, **156**, 96-103. https://doi.org/10.1016/j.clay.2018.01.035.
Cheng, L. (2012), "Innovative ground enhancement by improved microbially induced $CaCO_3$ precipitation technology", Ph.D. Dissertation; Murdoch University, Perth, Western Australia, Australia.
Cheng, L., Cord-Ruwisch, R. and Shahin, M.A. (2013), "Cementation of sand soil by microbially induced calcite precipitation at various degrees of saturation", *Can. Geotech. J.*, **50**, 81-90. https://doi.org/10.1139/cgj-2012-0023.
Cheng, L., Shahin, M.A. and Mujah, D. (2017), "Influence of key environmental conditions on microbially induced cementation for soil stabilization", *J. Geotech. Geoenviron. Eng.*, **143**(1), 04016083. https://doi.org/10.1061/(ASCE) GT.1943-5606.0001586.
Choi, S.G., Wang, K., Wen, Z. and Chu, J. (2017), "Mortar crack repair using microbial induced calcite precipitation method", *Cement Concrete Compos.*, **83**, 209-221. https://doi.org/10.1016/j.cemconcomp.2017.07.013.
Choi, S.G., Chu, J. and Kwon, T.H. (2019), "Effect of chemical concentrations on strength and crystal size of biocemented sand", *Geomech. Eng.*, **17**(5), 465-473. https://doi.org/10.12989/gae.2019.17.5.465.
Choi, S.G., Chang, I., Lee, M., Lee, J.H., Han, J.T. and Kwon, T.H. (2020), "Review on geotechnical engineering properties of sands treated by microbially induced calcium carbonate precipitation (MICP) and biopolymers", *Constr. Build. Mater.*, **246**, 118415. https://doi.org/10.1016/j.conbuildmat.2020.118415.
Connolly, J., Kaufman, M., Rothman, A., Gupta, R., Redden, G., Schuster, M., Colwell, F. and Gerlach, R. (2013), "Construction of two ureolytic model organisms for the study of microbially induced calcium carbonate precipitation", *J. Microbiol. Methods*, **94**, 290-299. https://doi.org/10.1016/j.mimet.2013.06.028.
Cui, M.J., Zheng, J.J., Zhang, R.J., Lai, H.J. and Zhang, J. (2017), "Influence of cementation level on the strength behaviour of bio-cemented sand", *Acta Geotech.*, **12**(5), 971-986. https://doi.org/10.1007/s11440-017-0574-9.
Cui, M.J., Zheng, Chu, J., Wu, C.C. and Lai, H.J. (2021), "Bio-mediated calcium carbonate precipitation and its effect on the shear behaviour of calcareous sand", *Acta Geotech.*, **16**(5), 1377-1389. https://doi.org/10.1007/s11440-020-01099-0.
Dadda, A., Geindreau, C., Emeriault, F., Rolland du Roscoat, S., Garandet, A., Sapin, L. and Esnaut Filet, A. (2017), "Characterization of microstructural and physical properties changes in biocemented sand using 3D X-ray microtomography", *Acta Geotech.*, **12**(5), 955-970. https://doi.org/10.1007/s11440-017-0578-5.
Darby, K.M., Hernandez, G.L., Dejong, J.T., Boulanger, R.W., Gomez, M.G. and Wilson, D.W. (2019), "Centrifuge Model testing of liquefaction mitigation via microbially induced calcite precipitation", *J. Geotech. Geoenviron. Eng.*, **145**, 1-13. https://doi.org/10.1061/(ASCE)GT.1943-5606.0002122.
Decho, A.W. (2010), "Overview of biopolymer-induced mineralization: What goes on in biofilms?", *Ecol. Eng.*, **36**, 137-144. https://doi.org/10.1016/j.ecoleng.2009.01.003.
Dejong, J.T., Fritzges, M.B. and Nüsslein, K. (2006), "Microbially induced cementation to control sand response to undrained shear", *J. Geotech. Geoenviron. Eng.*, **132**, 1381-1392. https://doi.org/10.1061/(ASCE)1090-0241(2006)132:11(1381).
Dejong, J.T., Mortensen, B.M., Martinez, B.C. and Nelson, D.C. (2010), "Bio-mediated soil improvement", *Ecol. Eng.*, **36**, 197-210. https://doi.org/10.1016/j.ecoleng.2008.12.029.
Dejong, J.T., Soga, K., Kavazanjian, E., Burns, S., Van Paassen, L.A., Al Qabany, A., Aydilek, A., Bang, S.S., Burbank, M., Caslake, L.F., Chen, C.Y., Cheng, X., Chu, J., Ciurli, S., Esnault-Filet, A., Fauriel, S., Hamdan, N., Hata, T., Inagaki, Y., Jefferis, S., Kuo, M., Laloui, L., Larrahondo, J., Manning, D.A.C., Martinez, B., Montoya, B.M., Nelson, D.C., Palomino, A., Renforth, P., Santamarina, J.C., Seagren, E.A., Tanyu, B., Tsesarsky, M. and Weaver, T. (2013), "Biogeochemical processes and geotechnical applications: Progress, opportunities and challenges", *Géotechnique*, **63**, 287-301. https://doi.org/10.1680/geot.SIP13.P.017.
Dejong, J.T., Martinez, B.C., Ginn, T.R., Hunt, C., Major, D. and Tanyu, B. (2014), "Development of a scaled repeated five-spot treatment model for examining microbial induced calcite precipitation feasibility in field applications", *Geotech. Test. J.*, **37**(3), 424-435. https://doi.org/10.1520/GTJ20130089.
Dhami, N.K., Reddy, M.S. and Mukherjee, A. (2013), "Biomineralization of calcium carbonate polymorphs by the bacterial strains isolated from calcareous sites", *J. Microbiol. Biotechnol.*, **23**, 707-714. https://doi.org/10.4014/jmb.1212.11087.
Do, J., Montoya, B.M. and Gabr, M.A. (2019), "Debonding of microbially induced carbonate precipitation-stabilized sand by shearing and erosion", *Geomech. Eng.*, **17**(5), 429-438. https://doi.org/10.12989/GAE.2019.17.5.429.
El-Latief, M.A.A., Ashour, M.B. and El-Tahrany, A.C. (2015). "Strengthening of the permeability of sandy soil by different grouting materials for seepage reduction", *Global J. Res Eng. Civ. Struct. Eng.*, **15**(3), 39-48.
Ercole, C., Bozzelli, P., Altieri, F., Cacchio, P. and Del Gallo, M. (2012), "Calcium carbonate mineralization: involvement of extracellular polymeric materials isolated from calcifying bacteria", *Microsc. Microanal.*, **18**(4), 829-839. https://doi.org/10.1017/S1431927612000426.
Eryürük K., Yang S., Suzuki D., Sakaguchi, I. and Katayama, A. (2015), "Effects of bentonite and yeast extract as nutrient on decrease in hydraulic conductivity of porous media due to $CaCO_3$ precipitation induced by *Sporosarcina pasteurii*", *J. Biosci. Bioeng.*, **120**, 411-418. https://doi.org/10.1016/j.jbiosc.2015.01.020.
Esnault Filet, A., Gutjahr, I., Garandet, A., Viglino, A., Beguin, R., Sibourg, O., Monnier, J.M., Martins, J., Oxarango, L., Spadini, L., Geindreau, C., Emeriault, F. and Castanier Perthuisot, S. (2019), "BOREAL, Bio-reinforcement of embankments by biocalcification", Digues Maritimes et Fluviales de Protection Contre les Inondations, Aix-en-Provence, France (in French).
Farah, T., Souli, H., Fleureau, J.M., Kermouche, G., Fry, J.J., Girard, B., Aelbrecht, D., Lambert, J. and Harkes, M. (2016), "Durability of bioclogging treatment of soils", *J. Geotech. Geoenviron. Eng.*, **142**(9), 04016040. https://doi.org/10.1061/(ASCE)GT.1943-5606.0001503.
Feng, K. and Montoya, B.M. (2016), "Influence of confinement and cementation level on the behavior of microbial-induced calcite precipitated Sands under monotonic drained loading", *J. Geotech. Geoenviron. Eng.*, **142**(1), 04015057. https://doi.org/10.1061/(ASCE)GT.1943-5606.0001379.
Feng, K. and Montoya, B.M. (2017), "Quantifying level of microbial-induced cementation for cyclically loaded sand", *J. Geotech. Geoenviron. Eng.*, **143**(6), 06017005. https://doi.org/10.1061/(ASCE)GT.1943-5606.0001682.
Gao, Y., Hang, L., He, J. and Chu, J. (2019), "Mechanical behaviour of biocemented sands at various treatment levels and relative densities", *Acta Geotech.*, **14**, 697-707.

https://doi.org/10.1007/s11440-018-0729-3.
Gat, D., Tsesarsky, M., Shamir, D. and Ronen, Z. (2014), "Accelerated microbial-induced $CaCO_3$ precipitation in a defined coculture of ureolytic and non-ureolytic bacteria", *Biogeosciences*, **11**(10), 2561-2569. https://doi.org/10.5194/bg-11-2561-2014.
Ghosh, T., Bhaduri, S., Montemagno, C. and Kumar, A. (2019), "*Sporosarcina pasteurii* can form nanoscale calcium carbonate crystals on cell surface", *PLoS One*, **14**, 1-15. https://doi.org/10.1371/journal.pone.0210339.
Gomez, M.G. and Dejong, J.T. (2017), "Engineering properties of bio-cementation improved sandy soils", *Proceedings of the Grouting 2017*, Honolulu, Hawaii, U.S.A., July.
Gomez, M.G., Dejong, J.T. and Anderson, C.M. (2018), "Effect of bio-cementation on geophysical and cone penetration measurements in sands", *Can. Geotech. J.*, **55**(11), 1632-1646. https://doi.org/10.1139/cgj-2017-0253.
Gowthaman, S., Nakashima, K., and Kawasaki S. (2021), "Freeze-thaw durability and shear responses of cemented slope soil treated by microbial induced carbonate precipitation", *Soils Found.*, **60**(4), 840-855. https://doi.org/10.1016/j.sandf.2020.05.012.
Haouzi, F., Esnault Filet, A. and Courcelles, B. (2019), "Performance studies of microbial induced calcite precipitation to prevent the erosion of internally unstable granular soils", *Proceedings of the GeoChina 2018*, Hangzhou, China, July.
Hataf, N. and Jamali, R. (2018), "Effect of fine-grain percent on soil strength properties improved by biological method", *Geomicrobiol. J.*, **35**, 695-703. https://doi.org/10.1080/01490451.2018.1454554.
Hussien, M.N. and Karray, M. (2016), "Shear wave velocity as a geotechnical parameter: An overview", *Can. Geotech. J.*, **53**(2), 252-272. https://doi.org/10.1139/cgj-2014-0524.
Imran, M.A., Nakashima, K., Evelpidou, N. and Kawasaki, S. (2019), "Factors affecting the urease activity of native ureolytic bacteria isolated from coastal areas", *Geomech. Eng.*, **17**(5), 421-427. https://doi.org/10.12989/gae.2019.17.5.421.
Ivanov, V. and Chu, J. (2008), "Applications of microorganisms to geotechnical engineering for bioclogging and biocementation of soil in situ", *Rev. Environ. Sci. Biotechnol.*, **7**, 139-153. https://doi.org/10.1007/s11157-007-9126-3.
Ivanov, V. (2010), *Environmental Microbiology for Engineers*, CRC Press, Taylor and Francis Group, Boca Raton, Florida, U.S.A
Jiang, N.J. and Soga, K. (2017), "The applicability of microbially induced calcite precipitation (MICP) for internal erosion control in gravel–sand mixtures", *Géotechnique*, **67**, 42-55. https://doi.org/10.1680/jgeot.15.p.182.
Jiang, N.J., Soga, K. and Kuo, M. (2017), "Microbially induced carbonate precipitation for seepage-induced internal erosion control in sand–clay mixtures", *J. Geotech. Geoenviron. Eng.*, **143**(3), 04016100. https://doi.org/10.1061/(asce)gt.1943-5606.0001559.
Kawaguchi, T. and Decho, A.W. (2002), "A laboratory investigation of cyanobacterial extracellular polymeric secretions (EPS) in influencing $CaCO_3$ polymorphism", *J. Cryst. Growth*, **240**, 230-235. https://doi.org/10.1016/S0022-0248(02)00918-1.
Lee, M., Gomez, M.G., El Kortbawi, M., and Ziotopoulou, K. (2020), "Examining the liquefaction resistance of lightly cemented sands using microbially induced calcite precipitation (MICP)", *Proceedings of the GeoCongress 2020*, Minneapolis, Minnesota, U.S.A., February.
Li, B. (2015), "Geotechnical properties of biocement treated sand and clay", Ph.D. Dissertation, Nanyang Technological University, Singapore.
Li, C., Yao, D., Liu, S., Zhou, T., Bai, S., Gao, Y. and Li, L. (2018), "Improvement of geomechanical properties of bio-remediated aeolian sand.", *Geomicrobiol. J.*, **35**, 132-140. https://doi.org/10.1080/01490451.2017.1338798.
Li, L., Wen, K., Li, C. and Amini, F. (2017), "FIB/SEM imaging of microbial induced calcite precipitation in sandy soil", *Microsc. Microanal.*, **23**, 310-311. https://doi.org/10.1017/S1431927617002239.
Liang, S., Chen, J., Niu, J., Gong, X. and Feng, D. (2019), "Using recycled calcium sources to solidify sandy soil through microbial induced carbonate precipitation", *Mar. Georesour. Geotec.*, **38**(4), 393-399. https://doi.org/10.1080/1064119X.2019.1575939.
Lin, H. (2016), "Microbial modification of soil for ground improvement", Ph.D. Dissertation, Lehigh University, Bethlehem, Pennsylvania, U.S.A.
Lin, H., Suleiman, M.T., Brown, D.G. and Kavazanjian, E. (2016), "Mechanical behavior of sands treated by microbially induced carbonate precipitation", *J. Geotech. Geoenviron. Eng.*, **142**, 1-13. https://doi.org/10.1061/(ASCE)GT.1943-5606.0001383.
Lin, H., Suleiman, M.T. and Brown, D.G. (2021), "Investigation of pore-scale $CaCO_3$ distributions and their effects on stiffness and permeability of sands treated by microbially induced carbonate precipitation (MICP)", *Soils Found.*, **60**(4), 944-961. https://doi.org/10.1016/j.sandf.2020.07.003.
Mahawish, A., Bouazza, A. and Gates, W.P. (2018), "Effect of particle size distribution on the bio-cementation of coarse aggregates", *Acta Geotech.*, **13**, 1019-1025. https://doi.org/10.1007/s11440-017-0604-7.
Martinez, B.C. and Dejong, J.T. (2009), "Bio-mediated soil improvement: Load transfer mechanisms at the micro- and macro- scales Brian", *Proceedings of the Workshop on Ground Improvement Technologies*, Orlando, Florida, U.S.A., March.
Martinez, B.C., Dejong, J.T., Ginn, T.R., Montoya, B.M., Barkouki, T.H., Hunt, C., Tanyu, B. and Major, D. (2013), "Experimental optimization of microbial-induced carbonate precipitation for soil improvement", *J. Geotech. Geoenviron. Eng.*, **139**, 587-598. https://doi.org/10.1061/(ASCE)GT.1943-5606.0000787.
Marzin, T., Desvages, B., Creppy, A., Lépine, L., Esnault-Filet, A. and Auradou, H. (2020), "Using Microfluidic set-up to determine the adsorption rate of *Sporosarcina pasteurii* bacteria on sandstone", *Transp. Porous Media*, **132**(2), 283-297. https://doi.org/10.1007/s11242-020-01391-3.
Montoya, B.M., Dejong, J.T., Boulanger, R.W., Wilson, D.W., Gerhard, R., Ganchenko, A. and Chou, J.C. (2012), "Liquefaction mitigation using microbial induced calcite precipitation", *Proceedings of the GeoCongress 2012*, Oakland, California, U.S.A.
Montoya, B.M., Dejong, J.T. and Boulanger, R.W. (2013), "Dynamic response of liquefiable sand improved by microbial-induced calcite precipitation", *Géotechnique*, **63**, 302-312. https://doi.org/10.1680/geot.SIP13.P.019.
Montoya, B.M. and Dejong, J.T. (2015), "Stress-strain behavior of sands cemented by microbially induced calcite precipitation", *J. Geotech. Geoenviron. Eng.*, **141**(6), 04015019. https://doi.org/10.1061/(ASCE)GT.1943-5606.0001302.
Mujah, D., Cheng, L. and Shahin, M.A. (2019), "Microstructural and geomechanical study on biocemented sand for optimization of MICP process", *J. Mater. Civ. Eng.*, **31**, 1-10. https://doi.org/10.1061/(ASCE)MT.1943-5533.0002660.
Nehrke, G. and Nouet, J. (2011), "Confocal Raman microscope mapping as a tool to describe different mineral and organic phases at high spatial resolution within marine biogenic carbonates: Case study on Nerita undata (Gastropoda, Neritopsina)", *Biogeosciences*, **8**(12), 3761-3769. https://doi.org/10.5194/bg-8-3761-2011.
O'Donnell, S.T., Rittmann, B.E. and Kavazanjian, E. (2017),

"MIDP: Liquefaction mitigation via microbial denitrification as a two-stage process. II: MICP", *J. Geotech. Geoenviron. Eng.*, **143**(12), 04017095. https://doi.org/10.1061/(ASCE)GT.1943-5606.0001806.

Omoregie, A.I., Ngu, L.H., Ong, D.E.L. and Nissom, P.M. (2019), "Low-cost cultivation of *Sporosarcina pasteurii* strain in food-grade yeast extract medium for microbially induced carbonate precipitation (MICP) application", *Biocatal. Agric. Biotechnol.*, **17**, 247-255. https://doi.org/10.1016/j.bcab.2018.11.030.

Porcino, D., Marcianò, V. and Granata, R. (2011), "Undrained cyclic response of a silicate-grouted sand for liquefaction mitigation purposes", *Geomech. Geoeng.*, **6**, 155-170. https://doi.org/10.1080/17486025.2011.560287.

Riveros, G.A., and Sadrekarimi, A. (2020), "Liquefaction resistance of Fraser river sand improved by a microbially-induced cementation", *Soil Dyn. Earthq. Eng.*, **131**, 1-14. https://doi.org/10.1016/j.soildyn.2020.106034.

Røyne, A., Phua, Y.J., Le, S.B., Eikjeland, I.G., Josefsen, K.D., Markussen, S., Myhr, A., Throne-Holst, H., Sikorski, P. and Wentzel, A. (2019), "Towards a low $CO_2$ emission building material employing bacterial metabolism (1/2): The bacterial system and prototype production", *PLoS One*, **14**(4). https://doi.org/10.1371/journal.pone.0212990.

Sarda, D., Choonia, H.S., Sarode, D.D. and Lele, S.S. (2009), "Biocalcification by Bacillus pasteurii urease: A novel application", *J. Ind. Microbiol. Biotechnol.*, **36**, 1111-1115. https://doi.org/10.1007/s10295-009-0581-4.

Schultze-Lam, S., Harauz, G. and Beveridge, T.J. (1992), "Participation of a cyanobacterial S layer in fine-grain mineral formation", *J. Bacteriol.*, **174**, 7971-7981. https://doi.org/10.1128/jb.174.24.7971-7981.1992.

Shahin, S., Montoya, B.M. and Gabr M.A. (2017), "Effect of microbial induced calcium carbonate precipitation on the performance of ponded coal ash", Association of State Dam Safety Officials, Inc., U.S.A.

Simatupang, M. and Okamura, M. (2017), "Liquefaction resistance of sand remediated with carbonate precipitation at different degrees of saturation during curing", *Soils Found.*, **57**, 619-631. https://doi.org/10.1016/j.sandf.2017.04.003.

Son, H.M., Kim, H.Y., Park, S.M. and Lee, H.K. (2018), "Ureolytic/Non-ureolytic bacteria co-cultured self-healing agent for cementitious materials crack repair", *Materials*. https://doi.org/10.3390/ma11050782.

Song, C., Elsworth, D., Zhi, S. and Wang, C. (2019), "The influence of particle morphology on microbially induced $CaCO_3$ clogging in granular media", *Mar. Georesour. Geotec.*, **39**(1), 74-81. https://doi.org/10.1080/1064119X.2019.1677828.

Soon, N.W., Lee, L.M., Khun, T.C. and Ling, H.S. (2013), "Improvements in engineering properties of soils through microbial-induced calcite precipitation", *KSCE J. Civ. Eng.*, **17**, 718-728. https://doi.org/10.1007/s12205-013-0149-8.

Soon, N.W., Lee, L.M., Khun, T.C. and Ling, H.S. (2014), "Factors affecting improvement in engineering properties of residual soil through microbial-induced calcite precipitation", *J. Geotech. Geoenviron. Eng.*, 140(5), 04014006. https://doi.org/10.1061/(ASCE)GT.1943-5606.0001089.

Stabnikov, V., Chu, J., Ivanov, V. and Li, Y. (2013), "Halotolerant, alkaliphilic urease-producing bacteria from different climate zones and their application for biocementation of sand", *World J. Microbiol. Biotechnol.*, **29**, 1453-1460. http://doi.org/10.1007/s11274-013-1309-1.

Stocks-Fischer, S., Galinat, J.K. and Bang, S.S. (1999), "Microbiological precipitation of $CaCO_3$", *Soil Biol. Biochem.*, **31**, 1563-1571. https://doi.org/10.1016/S0038-0717(99)00082-6.

Taïbi, S., Fleureau, J.-M., Hadiwardoyo, S. and Kheirbek-Saoud, S. (2008). "Small and large strain behaviour of an unsaturated compacted silt", *Eur. J. Environ. Civ. Eng.*, **12**(3), 203-228.

Terzis, D. and Laloui, L. (2019), "Cell-free soil bio-cementation with strength, dilatancy and fabric characterization", *Acta Geotech.*, **14**, 639-656. https://doi.org/10.1007/s11440-019-00764-3.

van Paassen L. (2009), "Biogrout: ground improvement by microbially induced carbonate precipitation", Ph.D. Dissertation, Delft University of Technology, The Netherlands.

Waller, J.T. (2011), "Influence of bio-cementation on shearing behavior in sand using X-ray computed tomography", Ph.D. Dissertation, University of California, Davis, California, U.S.A.

Wang, Y., Soga, K. and Jiang, N. (2017), "Microbial induced carbonate precipitation (MICP): the case for microscale perspective", *Proceedings of the 19th International Conference on Soil Mechanics and Geotechnical Engineering*, Seoul, Korea, December.

Wang, Y., Soga, K., Dejong, J.T. and Kabla, A.J. (2019), "A microfluidic chip and its use in characterising the particle-scale behaviour of microbial-induced carbonate precipitation (MICP)", *Géotechnique*, **69**, 1086-1094. https://doi.org/10.1680/jgeot.18.p.031.

Wang, Z., Zhang, N., Cai, G., Jin, Y., Ding, N. and Shen, D. (2017), "Review of ground improvement using microbial induced carbonate precipitation (MICP)", *Mar. Georesour. Geotec.*, **35**(8), 1135-1146. https://doi.org/10.1080/1064119X.2017.1297877.

Weil, M.H., Dejong, J.T., Martinez, B.C. and Mortensen, B.M. (2012), "Seismic and resistivity measurements for real-time monitoring of microbially induced calcite precipitation in sand", *Geotech. Test. J.*, **35**(2), 330-341. https://doi.org/10.1520/GTJ103365.

Wen, K., Li, Y., Liu, S., Bu, C. and Li, L. (2019), "Development of an improved immersing method to enhance microbial induced calcite precipitation treated sandy soil through multiple treatments in low cementation media concentration", *Geotech. Geol. Eng.*, **37**(2), 1015-1027. https://doi.org/10.1007/s10706-018-0669-6.

Whiffin, V.S. (2004), "Microbial $CaCO_3$ precipitation for the production of biocement", Ph.D. Dissertation, Murdoch University, Western Australia, Australia.

Whiffin, V.S., van Paassen, L. and Harkes, M. (2007), "Microbial carbonate precipitation as a soil improvement technique", *Geomicrobiol. J.*, **24**, 417-423. https://doi.org/10.1080/01490450701436505.

Wu, S. (2015), "Mitigation of liquefaction hazards using the combined biodesaturation and bioclogging method", Ph.D. Dissertation, Iowa State University, U.S.A.

Wu, S., Li, B. and Chu, J. (2021), "Stress-dilatancy behavior of MICP-treated sand", *Int. J. Geomech.*, **21**(3), 04020264-1-12. https://doi.org/10.1061/(ASCE)GM.1943-5622.0001923.

Xiao, P., Liu, H., Xiao, Y., Stuedlein, A.W. and Evans, T.M. (2018), "Liquefaction resistance of bio-cemented calcareous sand", *Soil Dyn. Earthq. Eng.*, **107**, 9-19. https://doi.org/10.1016/j.soildyn.2018.01.008.

Xiao, Y., Zhao, C., Sun Y., Wang, S., Wu, H., Chen, H. and Liu, H. (2020), "Compression behavior of MICP-treated sand with various gradations", *Acta Geotech.*, **16**(5), 1391-1400. https://doi.org/10.1007/s11440-020-01116-2.

Yasuhara, H., Neupane, D., Hayashi, K. and Okamura, M. (2012), "Experiments and predictions of physical properties of sand cemented by enzymatically-induced carbonate precipitation", *Soils Found.*, **52**, 539-549. https://doi.org/10.1016/j.sandf.2012.05.011.

Yu, T., Souli, H., Péchaud, Y. and Fleureau, J.M. (2020), "Optimizing protocols for microbial induced calcite precipitation (MICP) for soil improvement–a review", *Eur. J. Environ. Civ. Eng.*, 1-16.

https://doi.org/10.1080/19648189.2020.1755370.
Zhang, X., Chen, Y., Liu, H., Zhang, Z. and Ding, X. (2020), "Performance evaluation of a MICP-treated calcareous sandy foundation using shake table tests", *Soil Dyn. Earthq. Eng.*, https://doi.org/10.1016/j.soildyn.2019.105959.

*CC*